

High energy pA collisions in the color glass condensate approach

I. Gluon production and the Cronin effect

Jean-Paul Blaizot⁽¹⁾, François Gelis⁽¹⁾, Raju Venugopalan⁽²⁾

October 22, 2018

1. Service de Physique Théorique¹
Bât. 774, CEA/DSM/Saclay
91191, Gif-sur-Yvette Cedex, France
2. Physics Department
Brookhaven National Laboratory
Upton, NY 11973, USA

Abstract

We study gluon production in high energy proton-nucleus collisions in the semi-classical framework of the Color Glass Condensate. We develop a general formalism to compute gluon fields in covariant gauge to lowest order in the classical field of the proton and to all orders in the classical field of the nucleus. The use of the covariant gauge makes the diagrammatic interpretation of the solution more transparent. k_{\perp} -factorization holds to this order for gluon production – Our results for the gluon distribution are equivalent to the prior diagrammatic analysis of Kovchegov and Mueller. We also show that these results are equivalent to the computation of gluon production by Dumitru and McLerran in the Fock-Schwinger gauge. We demonstrate how the Cronin effect arises in this approach, and examine its behavior in the two extreme limits of a) no small- x quantum evolution, and b) fully saturated quantum evolution. In both cases, the formalism reduces to Glauber's formalism of multiple scatterings. We comment on the possible implications of this study for the interpretation of the recent results on Deuteron-Gold collisions at the Relativistic Heavy Ion Collider (RHIC).

¹URA 2306 du CNRS.

1 Introduction

The physics of high energy proton/deuteron–nucleus collisions has acquired new vigor with on-going experiments on Deuteron-Gold collisions at center of mass energies per nucleon of $\sqrt{s} = 200$ GeV being conducted at Brookhaven’s Relativistic Heavy Ion Collider (RHIC). First results from these experiments have already been submitted for publication and presented at conferences [1–4]. In the near future, CERN’s Large Hadron Collider (LHC) will study proton-nucleus collisions with center of mass energies per nucleon of $\sqrt{s} = 5.5$ TeV [5–7]. When one considers this important increase in the energy range for these collisions, it is interesting to examine how results from lower energy proton-nucleus collisions are modified both qualitatively and quantitatively as one goes to higher energies.

At very high energies, or small x values, the relevant parton densities in the proton and in nuclei grow very rapidly. If these densities are sufficiently large, the parton distributions may saturate, [8–10] leading to a qualitatively different behavior of the distributions. Saturation will occur sooner in nuclei than in protons because the large number of nucleons give rise to an enhanced parton density in the transverse plane by a factor $\sim A^{1/3}$. Proton-nucleus collisions therefore, for a wide energy range, provide an attractive physical environment wherein the proton probe may be considered as a dilute parton gas with properties that are believed to be well understood while the nucleus exists in a novel, saturated high density state. This latter state has been called a Color Glass Condensate (CGC) and its distinctive features have been extensively explored [11–30].

In this work, we will formulate a description of high energy proton-nucleus collisions within the CGC framework. In this framework, the proton and the nucleus are effectively described as static random sources of color charge on the light-cone. The leading contribution to particle production is obtained by calculating the classical Yang-Mills field created by these sources and then averaging over a random distribution. Thus one is led to solve the Yang-Mills equations in the presence of two number densities of color charges, $\rho_p(\mathbf{x}_\perp)$ and $\rho_A(\mathbf{x}_\perp)$ respectively for the proton and the nucleus, localized on the light-cone². One has

$$[D_\mu, F^{\mu\nu}] = J^\nu ,$$

where

$$J_a^\nu = g\delta^{\nu+}\delta(x^-)\rho_{p,a}(\mathbf{x}_\perp) + g\delta^{\nu-}\delta(x^+)\rho_{A,a}(\mathbf{x}_\perp) . \quad (1)$$

Operators calculated in this classical background field have to be averaged over weight functionals W_p and W_A – representing the distribution of the densities

²The validity of this approach is not obvious a priori – the motivations for this approach have been discussed extensively in the literature and we will not go into them here [31–37]. Here, it will be apparent only *a posteriori* – from its success in reproducing known results and its predictive power.

of color charges in the proton and nucleus respectively. One has then

$$\langle O \rangle = \int [D\rho_p][D\rho_A] W_p[x_0^p, \rho_p] W_A[x_0^A, \rho_A] O[\rho_p, \rho_A]. \quad (2)$$

This averaging procedure is essential in order to restore gauge invariance since $O[\rho_p, \rho_A]$ is computed in a particular gauge. The arguments x_0^p and x_0^A denote the scale in x separating the large x static sources from the small x dynamical fields. It is also through W_p and W_A that quantum effects, due to evolution with x of the light-cone wave functions of the target and projectile, are incorporated. The functionals W_p and W_A obey a Wilson renormalization group equation (often called the JIMWLK equation [15–27]), which governs their evolution with x_0^p and x_0^A . This equation reduces to the well-known BFKL equation in the low density or large transverse momentum limit. In this paper, we will explicitly show that the physical quantities relevant for proton-nucleus collisions can be related to correlators of Wilson lines, the quantum evolution of which can be studied thanks to the JIMWLK equation.

The first part of this work, on gluon production in pA collisions, will be presented in this paper. The second part, on quark production, will start from the solution of the Yang-Mills equations obtained in the present paper and will be discussed in an accompanying paper [38].

This paper is organized as follows. In section 2, we show how the Yang-Mills equations can be truncated systematically in order to obtain a coupled set of equations for the gauge fields to first order in the proton source density ρ_p and to all orders in the nuclear source density ρ_A . This approximation is valid as long as the parton densities in the proton remains small: this is of course the case at moderate collision energies, but also at very high collision energies albeit in a more restricted kinematical domain (not too far away from the fragmentation region of the proton). Gauge invariance is preserved, by construction, in this truncation. We explore the structure of these truncated equations and introduce a convenient diagrammatic expression for the gauge fields. The equations are solved explicitly in section 3. We obtain a compact expression for the gauge fields in terms of two distinct Wilson lines whose coefficients are shown to be simply related to the well known effective Lipatov vertex [39–42]. Classical gluon production is discussed in section 4. It is shown explicitly how the results can be written in a k_\perp -factorized form as the product of two k_\perp -dependent distributions times a factor proportional to the square of the Lipatov vertex. The results obtained in this fashion are compared to the results of Dumitru and McLerran [43] in Fock-Schwinger gauge and are shown to be identical. In section 5, we show how the Cronin effect arises in simple models with and without quantum evolution of the color charge densities. Readers interested in this topic alone may skip directly to section 5. Interpreting our results in light of the recent data from the BRAHMS experiment at RHIC for both central and forward rapidities [1], we find interesting ramifications for our understanding of the physics from both d-Au and Au-Au experiments at RHIC as well as for the future Heavy Ion experiments at CERN’s Large Hadron Collider (LHC). Various technical details are included in appendices A and B. Finally, we comment on the

relation of results in our approach to the Glauber multiple scattering formalism. Since this is somewhat outside the main thrust of this paper, we discuss it in a self-contained fashion in appendix C. We conclude in section 6 and set the stage for the results on quark production to be presented in [38].

Before we proceed further, we should point out that several results on gluon production in this paper are not new. They were first derived, in covariant gauge, by Kovchegov and Mueller [35] and subsequently refined in later papers [44,45]. These results were also derived, shortly after the work of Kovchegov and Mueller, by Dumitru and McLerran in the Fock-Schwinger or radiation gauge [43]. (We should also mention the work of Braun in a somewhat different approach [46].) Our derivation, albeit also in covariant gauge, follows a different tack from the Feynman diagram technique of Kovchegov and Mueller. We solve the Yang-Mills equations explicitly for the light-cone sources in Eq. 1. The expressions for the gauge fields are derived explicitly and one observes how the Lipatov vertex arises in this approach. We also show, for the first time, the exact equivalence between the approach of Kovchegov and Mueller with that of Dumitru and McLerran. Our results for the gauge fields are new and will be useful in deriving the result for quark production, which will be discussed in [38] (henceforth referred to as paper II). Our discussion of the Cronin effect is also, in part, known from previous work by us and other authors [47–52,45,53–55]. Our results in the “super-saturated” limit are new and help clarify the interpretation of the RHIC data. The fact that one recovers the Glauber multiple scattering picture in the case where the correlations of the color sources are Gaussian is well known [56–58] – however the formalism discussed here provides a systematic way to go beyond the limitations of the Glauber model by incorporating the non-Gaussian correlations that may arise via quantum evolution.

2 Yang-Mills equations

The Color Glass Condensate is a classical effective field theory which describes the physics of high energy, semi-hard processes in QCD. In this approach, one first solves the classical Yang-Mills equations in the presence of the light-cone sources ρ_p and ρ_A , next one computes the observable of interest in this classical field, and finally one averages over the sources ρ_p and ρ_A . For proton-nucleus collisions, one requires the solution of the gauge field to lowest order³ in the source density ρ_p of the proton and to all orders in the nuclear source density ρ_A . We shall write down in this section the truncated set of Yang-Mills equations to this order. We next show that these equations can be written in a compact form and explore their structure and their diagrammatic content. Solutions to the Yang-Mills equations will be discussed in the next section.

³Going beyond this approximation and solving the Yang-Mills equations to all orders in both sources has only been possible numerically so far [36,37,59–61].

2.1 Generalities and notations

The classical Yang-Mills equations read⁴:

$$[D_\mu, F^{\mu\nu}] = J^\nu . \quad (3)$$

J^ν is a color current which at lowest order in the sources ρ_p and ρ_A reads:

$$J_a^\nu = g\delta^{\nu+}\delta(x^-)\rho_{p,a}(\mathbf{x}_\perp) + g\delta^{\nu-}\delta(x^+)\rho_{A,a}(\mathbf{x}_\perp) . \quad (4)$$

ρ_p is the color source describing the proton, moving in the $+z$ direction at the speed of light. ρ_A is the color source describing the nucleus, moving in the opposite light-cone direction. These sources represent the number densities of color charges in the proton and nucleus respectively, which are Lorentz contracted to delta functions [31–33] $-\delta(x^\pm)$. In general, the current J_a^ν receives higher order corrections in ρ_p, ρ_A because it must be covariantly conserved:

$$[D_\nu, J^\nu] = 0 , \quad (5)$$

and the produced gauge field has a feedback on the current itself. Moreover, this system of equations is still under-determined because of gauge invariance. Here, we choose the Lorenz gauge:

$$\partial_\mu A^\mu = 0 . \quad (6)$$

Using this gauge condition, one can bring the Yang-Mills equations to the following form

$$\square A^\nu = J^\nu + ig[A_\mu, F^{\mu\nu} + \partial^\mu A^\nu] . \quad (7)$$

Since the commutator starts at least one order in $\rho_{p,A}$ after the gauge field itself, this form is appropriate for an expansion in powers of the color sources.

In this section where we deal with truncations of the Yang-Mills equations, it is convenient to introduce the following notations. For any quantity X , let us denote by $X_{(m,n)}$ the term of order $\rho_p^m \rho_A^n$ in its expansion in powers of the sources. We therefore have:

$$X = \sum_{m=0}^{+\infty} \sum_{n=0}^{+\infty} X_{(m,n)} . \quad (8)$$

Let us also denote by $X_{(0,\infty)}$ and $X_{(1,\infty)}$ the quantity X at order 0 and 1 in ρ_p and to all orders in ρ_A , i.e.:

$$\begin{aligned} X_{(0,\infty)} &\equiv \sum_{n=0}^{+\infty} X_{(0,n)} , \\ X_{(1,\infty)} &\equiv \sum_{n=0}^{+\infty} X_{(1,n)} . \end{aligned} \quad (9)$$

Thus, for pA collisions in a kinematical regime where the proton can be seen as a dilute object, we want to determine the component $A_{(1,\infty)}^\nu$ of the gauge field.

⁴By convention: $D^\mu \equiv \partial^\mu - igA^\mu$.

2.2 Order ρ_p^0

Before we proceed to consider the field generated in proton-nucleus collisions, let us first discuss the well-known case of the classical field of a nucleus (before the collision). If we first rewrite the Yang-Mills and current conservation equations to order ρ_p^0 , we have:

$$\begin{aligned}\square A_{(0,\infty)}^\nu &= J_{(0,\infty)}^\nu + ig[A_{(0,\infty)\mu}, F_{(0,\infty)}^{\mu\nu} + \partial^\mu A_{(0,\infty)}^\nu], \\ \partial_\mu J_{(0,\infty)}^\mu &= ig[A_{(0,\infty)\mu}, J_{(0,\infty)}^\mu].\end{aligned}\quad (10)$$

This system of equations can be solved iteratively to the appropriate order in ρ_A . Indeed, at any given step, the commutators of the r.h.s. always involve the gauge field obtained at the previous step. At order ρ_A^1 , we have simply:

$$\begin{aligned}J_{(0,1)}^\mu &= g\delta^{\mu-}\delta(x^+)\rho_A(\mathbf{x}_\perp), \\ \partial_\mu J_{(0,1)}^\mu &= 0, \\ \square A_{(0,1)}^\mu &= J_{(0,1)}^\mu.\end{aligned}\quad (11)$$

Note that the current conservation is automatically satisfied at this order, because J^μ has only a $-$ component that does not depend on x^- (hence⁵ $\partial_\mu J_{(0,1)}^\mu = \partial^+ J_{(0,1)}^- = 0$). The solution of the Yang-Mills equation is also trivial⁶:

$$A_{(0,1)}^\mu = -g\delta^{\mu-}\delta(x^+)\frac{1}{\nabla_\perp^2}\rho_A(\mathbf{x}_\perp).\quad (12)$$

Note that the field strength corresponding to this solution has only two non-vanishing components:

$$F_{(0,1)}^{i-} = -F_{(0,1)}^{-i} = \partial^i A_{(0,1)}^-.\quad (13)$$

At the order ρ_A^2 , the equations are:

$$\begin{aligned}\partial_\mu J_{(0,2)}^\mu &= ig[A_{(0,1)\mu}, J_{(0,1)}^\mu], \\ \square A_{(0,2)}^\nu &= J_{(0,2)}^\nu + ig[A_{(0,1)\mu}, F_{(0,1)}^{\mu\nu} + \partial^\mu A_{(0,1)}^\nu].\end{aligned}\quad (14)$$

Given the solution obtained at the first order, the commutator $[A_{(0,1)\mu}, J_{(0,1)}^\mu]$ that appears in the current conservation equation vanishes, and the solution is $J_{(0,2)}^\mu = 0$ if we impose that the current vanishes in the remote past. The same is true of the commutator $[A_{(0,1)\mu}, F_{(0,1)}^{\mu\nu} + \partial^\mu A_{(0,1)}^\nu]$, so that we have simply $\square A_{(0,2)}^\nu = 0$. Again, if we impose that the field vanishes in the remote past, we

⁵ $\partial^+ \equiv \partial/\partial x^-$, $\partial^- \equiv \partial/\partial x^+$.

⁶This notation is a convenient abuse of language. One should of course read:

$$\frac{1}{\nabla_\perp^2}\rho_A(\mathbf{x}_\perp) \equiv \int d^2\mathbf{y}_\perp \langle \mathbf{x}_\perp | \frac{1}{\nabla_\perp^2} | \mathbf{y}_\perp \rangle \rho_A(\mathbf{y}_\perp).$$

have $A_{(0,2)}^\nu = 0$. Therefore, the gauge field has no term of order $\rho_p^0 \rho_A^2$. These arguments can be trivially extended to any order in ρ_A , so that the solution at order $\rho_p^0 \rho_A^1$ is in fact valid to all orders in ρ_A :

$$\begin{aligned} J_{(0,\infty)}^\mu &= J_{(0,1)}^\mu = \delta^{\mu-} \delta(x^+) \rho_A(\mathbf{x}_\perp), \\ A_{(0,\infty)}^\mu &= A_{(0,1)}^\mu = -g \delta^{\mu-} \delta(x^+) \frac{1}{\nabla_\perp^2} \rho_A(\mathbf{x}_\perp). \end{aligned} \quad (15)$$

In section 3 and following, we will denote the field of the nucleus alone simply A_A^μ instead of $A_{(0,1)}^\mu$. Similarly, the field of the proton alone will be denoted A_p^μ instead of $A_{(1,0)}^\mu$.

2.3 Order ρ_p

We now come to the case of physical interest. At the order ρ_p^1 , the equations we need to solve are the following:

$$\begin{aligned} \square A_{(1,\infty)}^\nu &= J_{(1,\infty)}^\nu \\ &\quad + ig[A_{(1,\infty)\mu}, F_{(0,1)}^{\mu\nu} + \partial^\mu A_{(0,1)}^\nu] + ig[A_{(0,1)\mu}, F_{(1,\infty)}^{\mu\nu} + \partial^\mu A_{(1,\infty)}^\nu], \\ \partial_\mu J_{(1,\infty)}^\mu &= ig[A_{(1,\infty)\mu}, J_{(0,1)}^\mu] + ig[A_{(0,1)\mu}, J_{(1,\infty)}^\mu]. \end{aligned} \quad (16)$$

Let us begin with the equation for the current. We can make the reasonable assumption⁷ that $J_{(1,\infty)}^i = 0$, i.e. the current $J_{(1,\infty)}^\mu$ is purely longitudinal. This assumes that the sources that produce this current do not undergo any recoil, i.e. that they are eikonal light-cone sources. In addition, we require that the component $J_{(1,\infty)}^+$, which is a correction from interactions with the nucleus to the current produced by the proton, depends locally⁸ on $\rho_p(\mathbf{x}_\perp)$ (as was $J_{(1,0)}^+$). Since in the r.h.s. of the current conservation equation, the only term which is local in ρ_p is the term $ig[A_{(0,1)\mu}, J_{(1,\infty)}^\mu]$, we can in fact split this equation into separate equations for the + and - components of the current, as follows:

$$\begin{aligned} \partial^- J_{(1,\infty)}^+ &= ig[A_{(0,1)}^-, J_{(1,\infty)}^+], \\ \partial^+ J_{(1,\infty)}^- &= ig[A_{(1,\infty)}^+, J_{(0,1)}^-]. \end{aligned} \quad (17)$$

We can then write more explicitly the evolution equation for each component of the gauge field $A_{(1,\infty)}^\mu$, using all the information we know from the field at the previous order. For $A_{(1,\infty)}^+$, we get:

$$\square A_{(1,\infty)}^+ = J_{(1,\infty)}^+ + ig[A_{(0,1)}^-, \partial^+ A_{(1,\infty)}^+]. \quad (18)$$

For the transverse components $A_{(1,\infty)}^i$, we have the following equation:

$$\square A_{(1,\infty)}^i = ig[\partial^i A_{(0,1)}^-, A_{(1,\infty)}^+] - ig[A_{(0,1)}^-, \partial^i A_{(1,\infty)}^+] + 2ig[A_{(0,1)}^-, \partial^+ A_{(1,\infty)}^i]. \quad (19)$$

⁷The fact that we can find an exact solution of the Yang-Mills and current conservation equations under this assumption will justify it a posteriori.

⁸This means that $\rho_p(\mathbf{x}_\perp)$ cannot enter in $J_{(1,\infty)}^+(\mathbf{x}_\perp)$ via $(1/\nabla_\perp^2)\rho_p(\mathbf{x}_\perp)$.

And finally, the equation for $A_{(1,\infty)}^-$ is:

$$\begin{aligned} \square A_{(1,\infty)}^- &= J_{(1,\infty)}^- + ig[A_{(1,\infty)}^+, \partial^- A_{(0,1)}^-] + 2ig[A_{(1,\infty)}^i, \partial^i A_{(0,1)}^-] \\ &\quad + ig[A_{(0,1)}^-, F_{(1,\infty)}^{+-} + \partial^+ A_{(1,\infty)}^-] . \end{aligned} \quad (20)$$

This last equation can be made more explicit if we replace the strength tensor by its expression (to order ρ_p and all orders in ρ_A):

$$F_{(1,\infty)}^{+-} = \partial^+ A_{(1,\infty)}^- - \partial^- A_{(1,\infty)}^+ - ig[A_{(1,\infty)}^+, A_{(0,1)}^-] , \quad (21)$$

which leads to:

$$\begin{aligned} \square A_{(1,\infty)}^- &= J_{(1,\infty)}^- + ig[A_{(1,\infty)}^+, \partial^- A_{(0,1)}^-] - ig[A_{(0,1)}^-, \partial^- A_{(1,\infty)}^+] \\ &\quad + (ig)^2 [A_{(0,1)}^-, [A_{(1,\infty)}^+, A_{(0,1)}^-]] \\ &\quad + 2ig[A_{(1,\infty)}^i, \partial^i A_{(0,1)}^-] + 2ig[A_{(0,1)}^-, \partial^+ A_{(1,\infty)}^-] . \end{aligned} \quad (22)$$

2.4 Interpretation of the equations

In order to make the connection between the solution of the Yang-Mills equation and the perturbative diagrammatic expansion, it is useful to interpret the equations derived in the previous section in terms of Feynman diagrams. These equations can be simplified by first rewriting all the commutators in terms of matrices of the adjoint representation, as follows:

$$[A, B]_a = if^{abc} A_b B_c = - (T^b)_{ca} A_b B_c = [(A \cdot T)B]_a . \quad (23)$$

We can then exploit this compact notation to rewrite the current conservation and Yang-Mills equations of the previous subsection as follows:

$$\begin{aligned} (\partial^- - ig A_{(0,1)}^- \cdot T) J_{(1,\infty)}^+ &= 0 , \\ \partial^+ J_{(1,\infty)}^- &= ig (A_{(1,\infty)}^+ \cdot T) J_{(0,1)}^- , \end{aligned} \quad (24)$$

and

$$\begin{aligned} (\square - ig A_{(0,1)}^- \cdot T \partial^+) A_{(1,\infty)}^+ &= J_{(1,\infty)}^+ , \\ (\square - 2ig A_{(0,1)}^- \cdot T \partial^+) A_{(1,\infty)}^i &= -ig (A_{(0,1)}^- \cdot T) \partial^i A_{(1,\infty)}^+ \\ &\quad + ig (\partial^i A_{(0,1)}^- \cdot T) A_{(1,\infty)}^+ , \\ (\square - 2ig A_{(0,1)}^- \cdot T \partial^+) A_{(1,\infty)}^- &= J_{(1,\infty)}^- \\ &\quad - ig (A_{(0,1)}^- \cdot T) \partial^- A_{(1,\infty)}^+ + ig (\partial^- A_{(0,1)}^- \cdot T) A_{(1,\infty)}^+ \\ &\quad - (ig)^2 (A_{(0,1)}^- \cdot T)^2 A_{(1,\infty)}^+ - 2ig (\partial^i A_{(0,1)}^- \cdot T) A_{(1,\infty)}^i \end{aligned} \quad (25)$$

When writing these equations, we have collected in the l.h.s. all the homogeneous terms, and kept the inhomogeneous terms in the r.h.s. One then sees

that the structure of these equations requires that we solve them in a specific order: we need to first determine $J_{(1,\infty)}^+$, then $A_{(1,\infty)}^+$, $A_{(1,\infty)}^i$, $J_{(1,\infty)}^-$, and finally $A_{(1,\infty)}^-$. This is so because the quantities previously determined enter as source terms in the evolution equation for the latter quantities.

It is in fact easy to understand how the various components of the gauge field are coupled in these Yang-Mills equations by studying the structure of the gluon propagator in the color field $A_{(0,1)}^-$ created by the nucleus. Forgetting the source terms $J_{(1,\infty)}^\pm$ which are irrelevant in this discussion, we can formally write the field $A_{(1,\infty)}^\mu(x)$ at a “time” x^+ in terms of the field $A_{(1,\infty)}^\mu(y)$ at an earlier time x_0^+ via the retarded gluon propagator:

$$A_{(1,\infty)}^\mu(x) = \int_{y^+ = -\infty} dy^- d^2 \mathbf{y}_\perp G_R^{\mu\nu}(x, y) 2\partial_y^+ A_{(1,\infty)}^\nu(y). \quad (26)$$

where the integration is carried out on an hypersurface $y^+ = \text{const}$ (taken here to be infinitely remote in the past). $G_R^{\mu\nu}(x, y)$ is the retarded gluon propagator (in the presence of the background field $A_{(0,1)}^-$). Eq. (26) is not obvious and is derived in appendix A. In the following discussion, it will be convenient to consider the Fourier transform of the propagator, defined as follows:

$$G_R^{\mu\nu}(q, p) \equiv \int d^4 x d^4 y e^{iq \cdot x} e^{-ip \cdot y} G_R^{\mu\nu}(x, y). \quad (27)$$

The full propagator can be obtained by multiple insertions of the external field $A_{(0,1)}^-$ created by the nucleus. There are two possible insertions, corresponding respectively to a three gluon vertex or to a four gluon vertex, as illustrated in figure 1. The free propagator, proportional to $g^{\mu\nu}$, does not mix the various

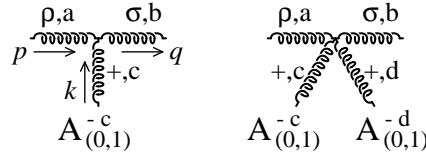


Figure 1: The three gluon vertex $\Gamma_{bac}^{\sigma\rho+}(q, p, k)$ and the four gluon vertex $\Gamma_{abcd}^{\sigma\rho++}(q, p, k_1, k_2)$ that can be inserted on the gluon propagator.

components $A_{(1,\infty)}^+$, $A_{(1,\infty)}^-$ and $A_{(1,\infty)}^i$ of the gauge field. This property however does not hold for the full propagator. In order to see this, let us consider the correction corresponding to the insertion of one external field $A_{(0,1)}^-$, via the 3-gluon vertex:

$$\delta G_R^{\mu\nu}(q, p) = G_R^{0\mu\sigma}(q) \left(\Gamma_{bac}^{\sigma\rho+}(q, p, k) A_{(0,1)}^{-c}(k) \right) G_R^{0\rho\nu}(p). \quad (28)$$

The vertex $\Gamma_{bac}^{\sigma\rho+}(q, p, k)$ is given by the usual QCD Feynman rules in the covariant gauge, and reads (see figure 1 for the direction of the momenta):

$$\Gamma_{bac}^{\sigma\rho+}(q, p, k) = gf^{abc} [g^{\rho\sigma}(p+q)^+ + g^{\sigma+}(-q-k)^\rho + g^{\rho+}(k-p)^\sigma] . \quad (29)$$

More explicitly, its components are given by:

$$\begin{aligned} \Gamma_{bac}^{+++}(q, p, k) &= 0 , \\ \Gamma_{bac}^{--+}(q, p, k) &= -g(p+q)^- f^{abc} , \\ \Gamma_{bac}^{+-+}(q, p, k) &= \Gamma_{bac}^{-++}(q, p, k) = gp^+ f^{abc} , \\ \Gamma_{bac}^{i++}(q, p, k) &= \Gamma_{bac}^{+i+}(q, p, k) = 0 , \\ \Gamma_{bac}^{-i+}(q, p, k) &= -g(q+k)^i f^{abc} , \\ \Gamma_{bac}^{i-+}(q, p, k) &= g(k-p)^i f^{abc} , \\ \Gamma_{bac}^{ij+}(q, p, k) &= 2gp^+ g^{ij} f^{abc} . \end{aligned} \quad (30)$$

In these expressions, we have used the fact that $k^+ = 0$ (because the background field $A_{(0,1)}^-$ does not depend on x^-). This means that all the components of $\delta G_R^{\mu\nu}$ are non-zero, except for δG_R^{++} , δG_R^{+i} and δG_R^{i+} . Looking back at eq. (26), this implies that all the transitions $A_{(1,\infty)}^\nu \rightarrow A_{(1,\infty)}^\mu$ are allowed, except for the following transitions:

$$\begin{aligned} A_{(1,\infty)}^- &\rightarrow A_{(1,\infty)}^+ , \\ A_{(1,\infty)}^- &\rightarrow A_{(1,\infty)}^i , \\ A_{(1,\infty)}^i &\rightarrow A_{(1,\infty)}^+ , \end{aligned} \quad (31)$$

which cannot happen. The insertion of the 4-gluon vertex does not change this conclusion. Indeed, the corresponding correction to the propagator is given by:

$$\delta G_R^{\prime\mu\nu}(q, p) = G_0^{\mu\sigma}(q) \left(\Gamma_{bacd}^{\sigma\rho++} A_{(0,1)c}^- A_{(0,1)d}^- \right) G_0^{\rho\nu}(p) , \quad (32)$$

with a vertex that reads:

$$\Gamma^{\sigma\rho++} = ig^2 \delta^{\rho-} \delta^{\sigma-} (T^c T^d + T^d T^c)_{ab} . \quad (33)$$

Therefore, only the component $\delta G_R^{\prime--}$ is non-zero. This corresponds to a transition $A_{(1,\infty)}^+ \rightarrow A_{(1,\infty)}^-$.

Our discussion thus far goes a long way towards explaining how the equations for $A_{(1,\infty)}^+$, $A_{(1,\infty)}^i$ and $A_{(1,\infty)}^-$ are nested and what the couplings between the various field components are. We note the following salient points:

- $A_{(1,\infty)}^+$ cannot be produced from $A_{(1,\infty)}^i$ or from $A_{(1,\infty)}^-$. Therefore, the equation for $A_{(1,\infty)}^+$ does not involve any other component of the field, and its only source term is the term in $J_{(1,\infty)}^+$. Moreover, the term in $ig(A_{(0,1)}^- \cdot T)\partial^+ A_{(1,\infty)}^+$ is the term that corresponds to the transition $A_{(1,\infty)}^+ \rightarrow A_{(1,\infty)}^+$ by insertion of one power of the background field $A_{(0,1)}^-$, i.e. to the vertex Γ^{+-+} .

- $A_{(1,\infty)}^i$ can be produced from $A_{(1,\infty)}^+$. Since there is no source term $J_{(1,\infty)}^i$, the inhomogeneous terms in the equation for $A_{(1,\infty)}^i$ corresponds to the vertex that is responsible for the transition $A_{(1,\infty)}^+ \rightarrow A_{(1,\infty)}^i$, i.e. Γ^{i-+} . The homogeneous term in this equation corresponds to the transition $A_{(1,\infty)}^i \rightarrow A_{(1,\infty)}^i$, i.e. to the vertex Γ^{ii+} .
- In addition to the source term associated with the current $J_{(1,\infty)}^-$, $A_{(1,\infty)}^-$ can be produced from $A_{(1,\infty)}^+$ (vertices Γ^{--+} and Γ^{---+}) or from $A_{(1,\infty)}^-$ (vertex Γ^{-i+}). The homogeneous term in the equation for $A_{(1,\infty)}^-$ corresponds to the transition $A_{(1,\infty)}^- \rightarrow A_{(1,\infty)}^-$, i.e. to the vertex Γ^{-++} .

One should note however that the equation for $A_{(1,\infty)}^-$, as written in eq. (25), does not quite fit with this interpretation. (Among other things, the homogeneous term is twice too large for this interpretation to hold.) However, this can be rescued by subtracting from the r.h.s. of this equation the quantity $ig[A_{(0,1)}^-, \partial_\mu A_{(1,\infty)}^\mu]$, which is zero according to the gauge condition we have chosen. After this subtraction has been performed, the equation for $A_{(1,\infty)}^-$ becomes:

$$\begin{aligned}
(\square - igA_{(0,1)}^- \cdot T \partial^+) A_{(1,\infty)}^- &= J_{(1,\infty)}^- \\
-2ig(A_{(0,1)}^- \cdot T) \partial^- A_{(1,\infty)}^+ - ig(\partial^- A_{(0,1)}^- \cdot T) A_{(1,\infty)}^+ &+ g^2(A_{(0,1)}^- \cdot T)^2 A_{(1,\infty)}^+ \\
-ig(A_{(0,1)}^- \cdot T) \partial^i A_{(1,\infty)}^i - 2ig(\partial^i A_{(0,1)}^- \cdot T) A_{(1,\infty)}^i &. \tag{34}
\end{aligned}$$

One now notes that all the terms in the equation correspond to the above interpretation.

2.5 Diagrammatic content of the equations

At this stage, it is possible to sketch the Feynman diagrams that correspond to the terms included into the solution of the Yang-Mills equations at this order. The simplest case is the diagram corresponding to the solution at order ρ_p^0 . Since the field $A_{(0,1)}^-$ is linear in the source ρ_A , we can represent it by the diagram of the figure 2.

The current $J_{(1,\infty)}^+$ is obtained by multiple scatterings of the source ρ_p in the field $A_{(0,1)}^-$, as illustrated by the diagram on the left of figure 3.

A typical contribution to $A_{(1,\infty)}^+$ is obtained by producing a gluon from the current $J_{(1,\infty)}^+$, and then by letting this gluon propagate through the background field $A_{(0,1)}^-$. This is illustrated by the diagram in the middle of figure 3. The field $A_{(1,\infty)}^i$ has a source term proportional to $A_{(1,\infty)}^+$ multiplied by a vertex Γ^{i-+} that enables the transition $A_{(1,\infty)}^+ \rightarrow A_{(1,\infty)}^i$. There cannot be more than one such vertex. Once formed, the field $A_{(1,\infty)}^i$ propagates in the background field $A_{(0,1)}^-$, as illustrated by the diagram on the right of figure 3.

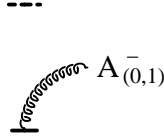


Figure 2: Diagrammatic representation of the field $A_{(0,1)}^-$. A solid boldface line represents one power of ρ_A , and a dashed boldface line represents one power of ρ_p .

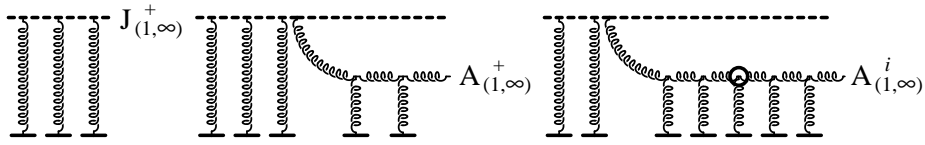


Figure 3: Diagrammatic representation of the current $J_{(1,\infty)}^+$ and of the fields $A_{(1,\infty)}^+$ and $A_{(1,\infty)}^i$. The circled vertex is the vertex Γ^{i-+} where the transition $A_{(1,\infty)}^+ \rightarrow A_{(1,\infty)}^i$ takes place.

There are several sources for the field $A_{(1,\infty)}^-$. One possible source is a direct transition $A_{(1,\infty)}^+ \rightarrow A_{(1,\infty)}^-$, as illustrated in figures 4 (there are a 3-gluon and a 4-gluon vertex for this transition). Another contribution to $A_{(1,\infty)}^-$ is due to the transition $A_{(1,\infty)}^+ \rightarrow A_{(1,\infty)}^i \rightarrow A_{(1,\infty)}^-$, as illustrated in figure 5. Finally, one last way to produce $A_{(1,\infty)}^-$ is via the source $J_{(1,\infty)}^-$, which requires the interaction of an $A_{(1,\infty)}^+$ with a source ρ_A . Note that this interaction is local in ρ_A . The diagrams contributing to $J_{(1,\infty)}^-$, as well as the corresponding contribution to $A_{(1,\infty)}^-$, are illustrated in figure 6.

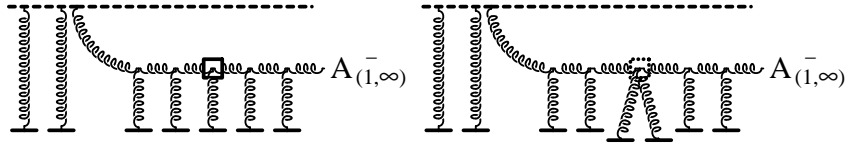


Figure 4: Contributions to $A_{(1,\infty)}^-$ by a direct transition $A_{(1,\infty)}^+ \rightarrow A_{(1,\infty)}^-$. Left: via the 3-point vertex; the boxed vertex is the vertex Γ^{--++} . Right: via the 4-point vertex; the dotted boxed vertex is the vertex Γ^{--++} .

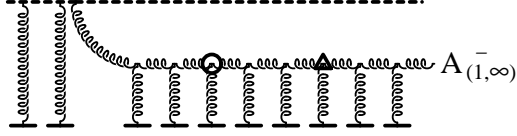


Figure 5: Contributions to $A_{(1,\infty)}^-$ by a transition $A_{(1,\infty)}^+ \rightarrow A_{(1,\infty)}^i \rightarrow A_{(1,\infty)}^-$. The triangular vertex is the vertex Γ^{-i+} .

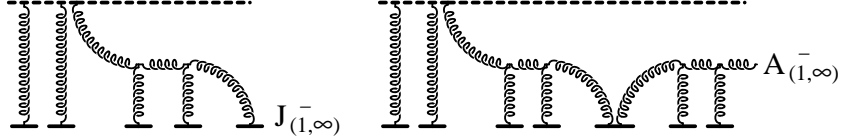


Figure 6: Contribution to $J_{(1,\infty)}^-$, and the corresponding contribution to $A_{(1,\infty)}^-$.

3 Solution of the gauge field equations

Now that we have written down the truncated set of coupled equations to lowest order ρ_p in the source density of the proton and to all orders in the source density of the nucleus, and understood the structure of these equations both analytically and diagrammatically, we are ready to solve the equations. This we will do in the order prescribed in the previous section. Since at this point, there is no risk of confusion, we can simplify our notations by removing the indices that indicate the orders in ρ_p and ρ_A . From now on, a quantity relative to the proton alone simply carries a subscript p , a quantity relative to the nucleus alone has a subscript A , and a quantity at order $(1, \infty)$ has no subscript at all. In particular, we have the following correspondence between the notations of the previous section, and those of the rest of the paper:

$$\begin{aligned} A_{(0,1)}^\mu &\longleftrightarrow A_A^\mu \quad , \quad A_{(1,0)}^\mu \longleftrightarrow A_p^\mu \quad , \\ A_{(1,\infty)}^\mu &\longleftrightarrow A^\mu \quad , \quad J_{(1,\infty)}^\mu \longleftrightarrow J^\mu \quad . \end{aligned} \quad (35)$$

3.1 Expression for the current J^+

In order to determine the source J^+ , we have to solve the equation:

$$(\partial^- - igA_A^- \cdot T)J^+ = 0 \quad , \quad (36)$$

with the initial condition $J^+(x^+ = -\infty) = J_p^+ = g\delta(x^-)\rho_p(\mathbf{x}_\perp)$. The solution can be expressed as:

$$J^+(x^+, x^-, \mathbf{x}_\perp) = gU(x^+, -\infty; \mathbf{x}_\perp)\delta(x^-)\rho_p(\mathbf{x}_\perp) \quad , \quad (37)$$

where

$$U(x_2^+, x_1^+; \mathbf{x}_\perp) \equiv \mathcal{P}_+ \exp \left[ig \int_{x_1^+}^{x_2^+} dz^+ A_A^-(z^+, \mathbf{x}_\perp) \cdot T \right] \quad (38)$$

is an adjoint Wilson line in the background field A_A^- (\mathcal{P}_+ denotes the ordering along x^+). Here A_A^- can be simply expressed in terms of the nuclear source density ρ_A through the expression given in eq. (15). Note that eq. (37) depends locally on $\rho_p(\mathbf{x}_\perp)$, but non-locally in $\rho_A(\mathbf{x}_\perp)$ (because it depends on ρ_A via the Weizäcker-Williams field A_A^-).

3.2 Expression for A^+

The next thing to do is to determine the field A^+ . It obeys the following equation:

$$(\square - igA_A^- \cdot T\partial^+)A^+ = J^+ . \quad (39)$$

We will go into the derivation of its solution in some detail because several subtle issues arise (regarding smearing of sources and the appearance of two different Wilson lines in the solution) that will be relevant for the discussion in this paper and in [38]. Using eq. (133) in appendix A, we can write the solution in terms of the source and of the initial condition at $y^+ = -\infty$ as follows:

$$\begin{aligned} A^+(x) &= \int d^4y G_R(x, y) J^+(y) \\ &+ \int_{y^+ = -\infty} dy^- d^2\mathbf{y}_\perp G_R(x, y) 2\partial_y^+ A^+(y) . \end{aligned} \quad (40)$$

where $G_R(x, y)$ is the retarded Green's function for the operator $\square - igA_A^- \cdot T\partial^+$, defined by:

$$\begin{aligned} (\square_x - igA_A^-(x) \cdot T\partial_x^+)G_R(x, y) &= \delta^{(4)}(x - y) , \\ \lim_{x^+ - y^+ \rightarrow 0^+} G_R(x, y) &= \frac{1}{2}\theta(x^- - y^-)\delta(\mathbf{x}_\perp - \mathbf{y}_\perp) , \\ G_R(x, y) &\propto \theta(x^+ - y^+) . \end{aligned} \quad (41)$$

The limit $x^+ \rightarrow y^+$ can be obtained from the free retarded propagator in the Feynman gauge⁹:

$$G_R^{0\mu\nu}(x, y) = -g^{\mu\nu} \int \frac{d^4k}{(2\pi)^4} \frac{e^{-ik \cdot (x-y)}}{k^2 + ik^+ \epsilon} = \frac{g^{\mu\nu}}{2\pi} \theta(x^+ - y^+) \theta(x^- - y^-) \delta((x - y)^2) . \quad (42)$$

⁹When the time difference goes to zero, the structure of the full propagator in x^+ becomes similar to that of the free propagator because there is not enough time for interactions with the background field to take place.

When $x^+ \rightarrow -\infty$, the gauge field must vanish because this is before the projectiles start contributing to the field. Therefore, we can take the second term in eq. (40) to be zero, and write simply:

$$A^+(x) = \int d^4y G_R(x, y) J^+(y). \quad (43)$$

The background field A_A^- is proportional to $\delta(x^+)$, but some expressions are ambiguous unless we regularize this delta function by giving it some small width. Therefore, we are going to replace in intermediate steps the $\delta(x^+)$ by a regular function $\delta_\epsilon(x^+)$ that is non-zero for $x^+ \in]0, \epsilon[$, and such that:

$$\int_0^\epsilon dx^+ \delta_\epsilon(x^+) = 1. \quad (44)$$

Note that the necessity of such a regularization is a peculiarity of the Lorenz gauge. Other oddities of this gauge will appear in the course of our calculation, which will naturally disappear from all physical quantities. Along with this regularization, we break down eq. (43) into three contributions, according to the value of y^+ :

$$\begin{aligned} A^+(x) &= \int_{-\infty}^0 dy^+ \int dy^- d\mathbf{y}_\perp G_R(x, y) J^+(y) \\ &+ \int_0^\epsilon dy^+ \int dy^- d\mathbf{y}_\perp G_R(x, y) J^+(y) \\ &+ \int_\epsilon^{x^+} dy^+ \int dy^- d\mathbf{y}_\perp G_R(x, y) J^+(y). \end{aligned} \quad (45)$$

We have assumed in this decomposition that $x^+ > \epsilon$. If this were not the case, some of the terms may be dropped.

Let us first discuss the expressions for the current in eq. (45). The expressions for the propagator will be discussed subsequently. In the first term, ($y^+ < 0$), we can replace the current J^+ by J_p^+ . In the intermediate term ($0 < y^+ < \epsilon$), we have¹⁰:

$$J^+(y) = g U(y^+, 0; \mathbf{y}_\perp) \delta(y^-) \rho_p(\mathbf{y}_\perp). \quad (46)$$

It is clear that the U which appears in this formula corresponds to a color rotation of the incoming sources due to interactions with the nucleus. In the third term ($y^+ > \epsilon$), we have:

$$J^+(y) = g U(\epsilon, 0; \mathbf{y}_\perp) \delta(y^-) \rho_p(\mathbf{y}_\perp). \quad (47)$$

We now consider the expressions for the propagators in the three terms in eq. (45). First we note the following convolution property that can be obtained by applying twice eq. (26):

$$G_R(x, y) = \int_{z^+ = \text{const}} dz^- d^2z_\perp G_R(x, z) 2\partial_z^+ G_R(z, y), \quad (48)$$

¹⁰Since the support of A_A^- is $0 < x^+ < \epsilon$, we have $U(x^+, -\infty; \mathbf{x}_\perp) = U(x^+, 0; \mathbf{x}_\perp)$.

valid for $y^+ < z^+ < x^+$ (see eq. (48)). This may be used in the first term of eq. (45), where $x^+ > \epsilon$ and $y^+ < 0$, in order to split the propagator into three pieces:

$$G_R(x, y) = \int_{v^+=\epsilon} dv^- d^2\mathbf{v}_\perp \int_{w^+=0} dw^- d^2\mathbf{w}_\perp G_R^0(x, v) 2\partial_v^+ G_R(v, w) 2\partial_w^+ G_R^0(w, y), \quad (49)$$

where we have used the fact that the propagator is a free propagator when its two endpoints are both in $[-\infty, 0]$ or in $[\epsilon, +\infty]$. Similarly, for the second term of eq. (45) ($x^+ > \epsilon$ and $0 < y^+ < \epsilon$), we split the propagator into two pieces:

$$G_R(x, y) = \int_{v^+=\epsilon} dv^- d^2\mathbf{v}_\perp G_R^0(x, v) 2\partial_v^+ G_R(v, y), \quad (50)$$

while in the third term ($x^+, y^+ > \epsilon$) we simply have:

$$G_R(x, y) = G_R^0(x, y). \quad (51)$$

We see that the only non-trivial propagator we need is the propagator connecting two points whose “times” x^+ and y^+ lie in the range $[0, \epsilon]$. In this case, the retarded propagator simply reads:

$$G_R(x, y) = \frac{1}{2}\theta(x^- - y^-)\delta(\mathbf{x}_\perp - \mathbf{y}_\perp)V(x^+, y^+; \mathbf{y}_\perp), \quad (52)$$

where:

$$V(x^+, y^+; \mathbf{y}_\perp) \equiv \mathcal{P}_+ \exp \left[i\frac{g}{2} \int_{y^+}^{x^+} dz^+ A_A^-(z^+, \mathbf{y}_\perp) \cdot T \right]. \quad (53)$$

This path ordered exponential is distinguished from the path ordered exponential U that we encountered previously by the factor of 1/2 that appears in the exponent. Notice further that

$$2\partial_x^+ G_R(x, y) = \delta(x^- - y^-)\delta(\mathbf{x}_\perp - \mathbf{y}_\perp)V(x^+, y^+; \mathbf{y}_\perp). \quad (54)$$

With the expressions for the currents and the propagators in the three distinct kinematical regions, we can now put together our expression for the gauge field in eq. (45). We first use the expression in eq. (54) for the propagator and the simple form for the current in the region $y^+ < 0$ to write the contribution to A^+ from this region as

$$g \int_{-\infty}^0 dy^+ \int_{y^-=0} d^2\mathbf{y}_\perp \int_{v^+=0} dv^- d^2\mathbf{v}_\perp G_R^0(x, v) V(\mathbf{v}_\perp) 2\partial_v^+ G_R^0(v, y) \rho_p(\mathbf{y}_\perp), \quad (55)$$

where we use a simpler notation for Wilson lines that run over the whole longitudinal extent of the nucleus:

$$V(\mathbf{x}_\perp) \equiv V(\epsilon, 0; \mathbf{x}_\perp) = V(+\infty, -\infty; \mathbf{x}_\perp). \quad (56)$$

Wherever possible, we have taken the limit $\epsilon \rightarrow 0$. Note that for the 1, i.e. the identity term, in the V path ordered exponential, one can trivially convolute the two free propagators and obtain:

$$g \int_{-\infty}^0 dy^+ \int_{y^-=0} d^2 \mathbf{y}_\perp G_R^0(x, y) \rho_p(\mathbf{y}_\perp), \quad (57)$$

which is nothing else but a piece of the field A_p^+ of the proton.

The contribution from the domain $y^+ \in [0, \epsilon]$ goes to zero when $\epsilon \rightarrow 0$. The only other contribution to A^+ is the one coming from the range $y^+ > \epsilon$:

$$g \int_0^{+\infty} dy^+ \int_{y^-=0} d^2 \mathbf{y}_\perp G_R^0(x, y) U(\mathbf{y}_\perp) \rho_p(\mathbf{y}_\perp). \quad (58)$$

The 1 in the ordered exponential U gives the second half of A_p^+ .

We can now combine the above results to write the complete solution for $A^+(x)$ in the region where $x^+ > 0$:

$$\begin{aligned} A^+(x) &= g \int_{-\infty}^0 dy^+ \int_{y^-=0} d^2 \mathbf{y}_\perp \int_{v^+=0} dv^- d^2 \mathbf{v}_\perp G_R^0(x, v) V(\mathbf{v}_\perp) 2\partial_v^+ G_R^0(v, y) \rho_p(\mathbf{y}_\perp) \\ &+ g \int_0^{+\infty} dy^+ \int_{y^-=0} d^2 \mathbf{y}_\perp G_R^0(x, y) U(\mathbf{y}_\perp) \rho_p(\mathbf{y}_\perp). \end{aligned} \quad (59)$$

Physically, this result made of only two terms suggests the following. In a collision at very high energy, the proton must emit the gluon either before or after hitting the nucleus. Emitting the gluon during the collision with the nucleus is very unlikely at high energy because of Lorentz contraction of longitudinal distances. (Such a process is suppressed by at least one power of the inverse collision energy.) Note however that, rather surprisingly, both path ordered exponentials U and V contribute to the expression of the gauge field. Naively, we would have believed only the contribution from the color rotation of the sources, the U 's would have been relevant; the V contribution, from the particular form of the propagator in this gauge, is unexpected. We will see that our intuitive expectations will be restored when we compute the gluon distribution¹¹.

In this derivation of A^+ , we rightly assumed throughout that $x^+ > \epsilon$. However, for later use in the calculation of A^i and A^- , we need also the value of $A^+(x)$ for $x^+ \in [0, \epsilon]$. Only the term where the gluon is emitted before the interaction of the proton with the nucleus can contribute here, and the last free propagator does not appear. We obtain,

$$A^+(0 < x^+ < \epsilon) = g \int_{-\infty}^0 dy^+ \int_{y^-=0} d^2 \mathbf{y}_\perp V(x^+, 0; \mathbf{x}_\perp) G_R^0(x, y) \rho_p(\mathbf{y}_\perp). \quad (60)$$

¹¹Albeit, further surprises await when we consider quark production [38].

It is also useful to compute the Fourier transform¹² of the field $A^+(x)$, for which we obtain¹³

$$\begin{aligned}
A^+(q) &= A_p^+(q) \\
&+ \frac{ig}{(q^- + i\epsilon)(q^2 + iq^+\epsilon)} \int d^2\mathbf{y}_\perp e^{-iq_\perp \cdot \mathbf{y}_\perp} [U(\mathbf{y}_\perp) - 1] \rho_p(\mathbf{y}_\perp) \\
&- \frac{ig 2q^+}{q^2 + iq^+\epsilon} \int d^2\mathbf{y}_\perp d^2\mathbf{v}_\perp \frac{d^2\mathbf{k}_\perp}{(2\pi)^2} e^{i(\mathbf{k}_\perp - \mathbf{q}_\perp) \cdot \mathbf{v}_\perp} \frac{[V(\mathbf{v}_\perp) - 1]}{\mathbf{k}_\perp^2} e^{-i\mathbf{k}_\perp \cdot \mathbf{y}_\perp} \rho_p(\mathbf{y}_\perp).
\end{aligned} \tag{61}$$

This expression can also be put in the more compact form

$$\begin{aligned}
A^+(q) &= A_p^+(q) \\
&+ \frac{ig}{q^2 + iq^+\epsilon} \int \frac{d^2\mathbf{k}_{1\perp}}{(2\pi)^2} \left\{ \frac{-k_{1\perp}^2}{q^- + i\epsilon} [U(\mathbf{k}_{2\perp}) - (2\pi)^2 \delta(\mathbf{k}_{2\perp})] \right. \\
&\quad \left. + 2q^+ [V(\mathbf{k}_{2\perp}) - (2\pi)^2 \delta(\mathbf{k}_{2\perp})] \right\} \frac{\rho_1(\mathbf{k}_{1\perp})}{k_{1\perp}^2}, \tag{62}
\end{aligned}$$

with the following notations:

$$\begin{aligned}
\mathbf{k}_{2\perp} &\equiv \mathbf{q}_\perp - \mathbf{k}_{1\perp}, \\
U(\mathbf{k}_\perp) &\equiv \int d^2\mathbf{x}_\perp e^{-i\mathbf{k}_\perp \cdot \mathbf{x}_\perp} U(\mathbf{x}_\perp), \\
V(\mathbf{k}_\perp) &\equiv \int d^2\mathbf{x}_\perp e^{-i\mathbf{k}_\perp \cdot \mathbf{x}_\perp} V(\mathbf{x}_\perp), \\
\rho_p(\mathbf{k}_\perp) &\equiv \int d^2\mathbf{x}_\perp e^{-i\mathbf{k}_\perp \cdot \mathbf{x}_\perp} \rho_p(\mathbf{x}_\perp).
\end{aligned} \tag{63}$$

When we expand the path ordered exponentials to first order in A_A^- , we recover the solution by Kovchegov and Rischke [33] for the gauge field to lowest order in *both* sources:

$$q^2 A_{(1,1)}^+(q) = -g^3 \int \frac{d^2\mathbf{k}_{1\perp}}{(2\pi)^2} \left[q^+ - \frac{k_{1\perp}^2}{q^-} \right] \frac{\rho_A(\mathbf{k}_{2\perp}) \cdot T \rho_p(\mathbf{k}_{1\perp})}{k_{2\perp}^2 k_{1\perp}^2}. \tag{64}$$

Note that it only thanks to the fact that the Wilson line V has a factor 1/2 in its exponent that this lowest order result is correctly reproduced.

3.3 Expression for A^i

Since $A^i(x^+ = -\infty) = 0$, the component A^i of the field can be expressed as:

$$A^i(x) = \int d^4v D_R(x, v) J^i(v), \tag{65}$$

¹²We do not use a special symbol for Fourier transforms, since the context makes obvious what object we are dealing with.

¹³When computing this Fourier transform, one must remember that eq. (59) is not valid for $x^+ < 0$. In the region $x^+ < 0$, we simply have $A^+(x) = A_p^+(x)$.

where D_R is the retarded Green's function of the operator ¹⁴ $\square - 2igA_A^- \cdot T\partial^+$:

$$(\square_x - 2igA_A^-(x) \cdot T\partial_x^+)D_R(x, y) = \delta^{(4)}(x - y), \quad (66)$$

and where we denote

$$J^i(x) \equiv ig \left[(\partial^i A_A^-(x) \cdot T)A^+(x) - (A_A^-(x) \cdot T)\partial^i A^+(x) \right]. \quad (67)$$

Note that $J^i(x)$ is non-zero only for $x^+ \in [0, \epsilon]$ because of the proportionality to the field $A_A^-(x)$. The propagator D_R is almost the same as G_R : the only difference is that the ordered exponential V is replaced by a U (with the same arguments) in the region of interaction with A_A^- . It is easy to check that the propagator $D_R(x, v)$ connecting a point in the interaction region ($v^+ \in [0, \epsilon]$) and a point after the interaction region ($x^+ > \epsilon$) is given by:

$$D_R(x, v) = G_R^0(x, v)U(\epsilon, v^+; \mathbf{v}_\perp). \quad (68)$$

We need also eq. (60), which we can rewrite as follows:

$$\begin{aligned} A^+(x) &= gV(x^+, 0; \mathbf{x}_\perp) \int_{-\infty}^0 dy^+ \int_{y^-=0} d^2\mathbf{y}_\perp G_R^0(x, y) \rho_p(\mathbf{y}_\perp) \\ &= V(x^+, 0; \mathbf{x}_\perp) A_p^+(x). \end{aligned} \quad (69)$$

We can now put together all the ingredients in order to obtain,

$$\begin{aligned} A^i(x) &= ig \int_0^\epsilon dv^+ dv^- d^2\mathbf{v}_\perp G_{0R}(x, v) U(\epsilon, v^+; \mathbf{v}_\perp) \\ &\quad \times \left[(\partial_v^i A_A^-(v) \cdot T)V(v^+, 0; \mathbf{v}_\perp) A_p^+(v) \right. \\ &\quad \left. - (A_A^-(v) \cdot T)\partial_v^i (V(v^+, 0; \mathbf{v}_\perp) A_p^+(v)) \right]. \end{aligned} \quad (70)$$

The Fourier transform of this expression is given by

$$\begin{aligned} A^i(q) &= \frac{ig}{q^2 + iq^+\epsilon} \int_0^\epsilon dv^+ dv^- d^2\mathbf{v}_\perp e^{iq^+v} U(\epsilon, v^+; \mathbf{v}_\perp) \\ &\quad \times \left[(\partial_v^i A_A^-(v) \cdot T)V(v^+, 0; \mathbf{v}_\perp) A_p^+(v) \right. \\ &\quad \left. - (A_A^-(v) \cdot T)\partial_v^i (V(v^+, 0; \mathbf{v}_\perp) A_p^+(v)) \right]. \end{aligned} \quad (71)$$

At this stage, in order to further simplify our result, we must find a way to deal with the convolution of a U and a V . Using the results justified in appendix B, we can write this expression as

$$\begin{aligned} A^i(q) &= \frac{2}{q^2 + iq^+\epsilon} \int dv^- d^2\mathbf{v}_\perp e^{i(q^+v^- - \mathbf{q}_\perp \cdot \mathbf{v}_\perp)} \\ &\quad \times \left\{ (V(\mathbf{v}_\perp) - U(\mathbf{v}_\perp)) \partial_v^i A_p^+(v) + (\partial_v^i V(\mathbf{v}_\perp)) A_p^+(v) \right\}. \end{aligned} \quad (72)$$

¹⁴The factor of 2 in eq. (66) is what distinguishes D_R from the propagator G_R in the previous subsection – see eq. (41).

A final simplification occurs after writing the terms on the r.h.s in terms of their Fourier components,

$$A^i(q) = \frac{2ig}{q^2 + iq^+\epsilon} \int \frac{d^2\mathbf{k}_{1\perp}}{(2\pi)^2} \left\{ k_1^i (V(\mathbf{k}_{2\perp}) - U(\mathbf{k}_{2\perp})) + k_2^i V(\mathbf{k}_{2\perp}) \right\} \frac{\rho_p(\mathbf{k}_{1\perp})}{k_{1\perp}^2}. \quad (73)$$

Expanding the time-ordered exponentials to first order in the background field A_A^- , we recover the lowest order solution of Kovchegov and Rischke [33] for the transverse components of the gauge field at that order,

$$q^2 A_{(1,1)}^i(q) = -g^3 \int \frac{d^2\mathbf{k}_{1\perp}}{(2\pi)^2} [k_2^i - k_1^i] \frac{\rho_A(\mathbf{k}_{2\perp}) \cdot T}{k_{2\perp}^2} \frac{\rho_p(\mathbf{k}_{1\perp})}{k_{1\perp}^2}. \quad (74)$$

3.4 Expression for A^-

One way of determining A^- would be to solve its equation of motion with the appropriate source terms. Since there are several source terms, this procedure is somewhat lengthy. It is much easier instead to obtain the final component of the field A^μ from the gauge condition. In Fourier space, the latter reads as follows:

$$q^- A^+(q) + q^+ A^-(q) - \mathbf{q}_\perp \cdot \mathbf{A}_\perp(q) = 0. \quad (75)$$

This further implies that

$$A^-(q) = \frac{1}{q^+} [\mathbf{q}_\perp \cdot \mathbf{A}_\perp(q) - q^- A^+(q)]. \quad (76)$$

Substituting our results for A^+ and A^i from the previous two subsections, we obtain,

$$A^-(q) = \frac{ig}{q^2 + iq^+\epsilon} \int \frac{d^2\mathbf{k}_{1\perp}}{(2\pi)^2} \left\{ \left(\frac{k_{2\perp}^2 - q_\perp^2}{q^+} \right) [U(\mathbf{k}_{2\perp}) - (2\pi)^2 \delta(\mathbf{k}_{2\perp})] \right. \\ \left. + \left(2 \frac{q_\perp^2}{q^+} - 2q^- \right) [V(\mathbf{k}_{2\perp}) - (2\pi)^2 \delta(\mathbf{k}_{2\perp})] \right\} \frac{\rho_p(\mathbf{k}_{1\perp})}{k_{1\perp}^2}. \quad (77)$$

At order 0 in ρ_A , this expression is zero as expected. When we expand the time-ordered exponentials to first order in this formula, we again recover the known lowest order result [33],

$$q^2 A_{(1,1)}^-(q) = -g^3 \int \frac{d^2\mathbf{k}_{1\perp}}{(2\pi)^2} \left[\frac{k_{2\perp}^2}{q^+} - q^- \right] \frac{\rho_A(\mathbf{k}_{2\perp}) \cdot T}{k_{2\perp}^2} \frac{\rho_p(\mathbf{k}_{1\perp})}{k_{1\perp}^2}. \quad (78)$$

3.5 Summary of results for A^μ

We can now collect our results for the components of the field A^μ and examine these more closely. By construction, this solution obeys $\partial_\mu A^\mu = 0$. We have

also checked that it has the correct lowest order limit. It is useful to put this solution in the following compact form:

$$\begin{aligned}
A^\mu(q) &= A_p^\mu(q) \\
&+ \frac{ig}{q^2 + iq^+\epsilon} \int \frac{d^2\mathbf{k}_{1\perp}}{(2\pi)^2} \left\{ C_U^\mu(q, \mathbf{k}_{1\perp}) [U(\mathbf{k}_{2\perp}) - (2\pi)^2\delta(\mathbf{k}_{2\perp})] \right. \\
&\quad \left. + C_V^\mu(q) [V(\mathbf{k}_{2\perp}) - (2\pi)^2\delta(\mathbf{k}_{2\perp})] \right\} \frac{\rho_p(\mathbf{k}_{1\perp})}{k_{1\perp}^2}, \quad (79)
\end{aligned}$$

where we have defined the 4-vectors $C_{U,V}^\mu$ as follows,

$$\begin{aligned}
C_U^+(q, \mathbf{k}_{1\perp}) &\equiv -\frac{k_{1\perp}^2}{q^- + i\epsilon}, \quad C_U^-(q, \mathbf{k}_{1\perp}) \equiv \frac{k_{2\perp}^2 - q_\perp^2}{q^+}, \quad C_U^i(q, \mathbf{k}_{1\perp}) \equiv -2k_1^i, \\
C_V^+(q) &\equiv 2q^+ \quad , \quad C_V^-(q) \equiv 2\frac{q_\perp^2}{q^+} - 2q^- \quad , \quad C_V^i \equiv 2q^i. \quad (80)
\end{aligned}$$

These coefficients are simply related to the well known Lipatov effective vertex [39–42] C_L^μ through the relation $C_L^\mu = C_U^\mu + \frac{1}{2}C_V^\mu$. For any momentum q , these 4-vectors satisfy

$$q \cdot C_U = q \cdot C_V = 0, \quad (81)$$

which ensures that the covariant gauge condition is trivially verified. Moreover, for a momentum q *on-shell* ($2q^+q^- = q_\perp^2$), we have the following additional properties:

$$\begin{aligned}
C_U \cdot C_V &= C_V^2 = 0, \\
C_U^2 &= -4\frac{k_{1\perp}^2 k_{2\perp}^2}{q_\perp^2} = C_L^2. \quad (82)
\end{aligned}$$

Remarkably, this ensures that when we use this solution in order to compute the production of on-shell gluons, we get only the correlator $\langle UU^\dagger \rangle$ (the mixed correlators $\langle UV^\dagger \rangle$ and $\langle VU^\dagger \rangle$, as well as $\langle VV^\dagger \rangle$, do not appear). Moreover the non-zero scalar product C_U^2 is the square of the ordinary Lipatov vertex. This result suggests, as we will prove in the next section, that we likely have the property of k_\perp -factorization for gluon production in pA.

4 Classical gluon production in pA collisions

4.1 k_\perp -factorization in gluon production

From the results derived in the previous section, it is fairly easy now to derive the average multiplicity of gluons produced in pA collisions, to all orders in the source describing the nucleus. Using standard reduction formulas, the gluon production amplitude is given in the classical approximation by:

$$\mathcal{M}_\lambda(\mathbf{q}) = q^2 A^\mu(q) \epsilon_\mu^{(\lambda)}(\mathbf{q}), \quad (83)$$

where $\epsilon_\mu^{(\lambda)}(\mathbf{q})$ is the polarization vector for a gluon of 3-momentum \mathbf{q} in the polarization state λ . As usual, what this formula tells us is that we need to Fourier transform the gauge field, amputate the last free propagator (that's what the q^2 prefactor does), put the result on shell, and project on the appropriate polarization vector. When we square this amplitude, we can sum over all four polarization states including the two non physical ones. Indeed, the property $q_\mu A^\mu = 0$ ensures that the longitudinal polarization states are not going to contribute to the result. We can therefore use the identity,

$$\sum_\lambda \epsilon_\mu^{(\lambda)}(\mathbf{q}) \epsilon_\nu^{(\lambda)*}(\mathbf{q}) = -g_{\mu\nu}. \quad (84)$$

The average number of gluons produced in a collision is given by the relation

$$\begin{aligned} \overline{N}_g &= \int \frac{d^3\mathbf{q}}{(2\pi)^3 2E_q} \sum_\lambda \langle |\mathcal{M}_\lambda(\mathbf{q})|^2 \rangle \\ &= -g^2 \int \frac{d^3\mathbf{q}}{(2\pi)^3 2E_q} \frac{d^2\mathbf{k}_{1\perp}}{(2\pi)^2} \frac{d^2\mathbf{k}'_{1\perp}}{(2\pi)^2} \frac{C_U(q, \mathbf{k}_{1\perp}) \cdot C_U(q, \mathbf{k}'_{1\perp})}{k_{1\perp}^2 k'_{1\perp}{}^2} \\ &\quad \times \langle \rho_{p,a}^\dagger(\mathbf{k}_{1\perp}) \rho_{p,a'}(\mathbf{k}'_{1\perp}) \rangle \langle U^\dagger(\mathbf{k}_{2\perp}) U(\mathbf{k}'_{2\perp}) \rangle_{aa'}, \quad (85) \end{aligned}$$

where $\langle \dots \rangle$ denotes the average over the color sources. Note that the field $A_p^+(q)$ of the proton alone does not contribute to on-shell gluon production. In order to rewrite this expression in a more intuitive way, let us first express the correlator of the proton sources ρ_p in terms of the unintegrated gluon distribution in the proton:

$$\begin{aligned} g^2 \langle \rho_{p,a}^\dagger(\mathbf{k}_{1\perp}) \rho_{p,a'}(\mathbf{k}'_{1\perp}) \rangle &= \\ &= \frac{\delta^{aa'}}{\pi d_A} \left[\frac{\mathbf{k}_{1\perp} + \mathbf{k}'_{1\perp}}{2} \right]^2 \int_{\mathbf{X}_\perp} e^{i(\mathbf{k}_{1\perp} - \mathbf{k}'_{1\perp}) \cdot \mathbf{X}_\perp} \frac{d\varphi_p(\frac{\mathbf{k}_{1\perp} + \mathbf{k}'_{1\perp}}{2} | \mathbf{X}_\perp)}{d^2\mathbf{X}_\perp}. \quad (86) \end{aligned}$$

The integration over \mathbf{X}_\perp runs over the transverse profile of the proton. $d_A \equiv N^2 - 1$ is the dimension of the adjoint representation of $SU(N)$, and $d\varphi_p/d^2\mathbf{X}_\perp$ is the number of gluons per unit area and unit of transverse momentum in the proton (i.e. the proton non-integrated gluon distribution per unit area). Note that the impact parameter does not appear here simply because we chose the origin of transverse coordinates at the center of the proton (\mathbf{b} will therefore appear in the correlator involving the U 's). This correlator can be approximated further if we realize that the support for the integration over \mathbf{X}_\perp is the transverse area of the proton, a domain of typical size $1/\Lambda_{QCD}$. This means that the difference $\mathbf{k}_{1\perp} - \mathbf{k}'_{1\perp}$, which is the conjugate variable of \mathbf{X}_\perp , is at most of order Λ_{QCD} . Therefore, as long as we are interested in transverse momenta much larger than Λ_{QCD} , we can always approximate $\mathbf{k}_{1\perp} \approx \mathbf{k}'_{1\perp}$. In particular, we can write:

$$g^2 \langle \rho_{p,a}^\dagger(\mathbf{k}_{1\perp}) \rho_{p,a'}(\mathbf{k}'_{1\perp}) \rangle = \frac{\delta^{aa'}}{\pi d_A} \mathbf{k}_{1\perp}^2 \int_{\mathbf{X}_\perp} e^{i(\mathbf{k}_{1\perp} - \mathbf{k}'_{1\perp}) \cdot \mathbf{X}_\perp} \frac{d\varphi_p(\mathbf{k}_{1\perp} | \mathbf{X}_\perp)}{d^2\mathbf{X}_\perp}. \quad (87)$$

We will also neglect the difference $\mathbf{k}_{1\perp} - \mathbf{k}'_{1\perp}$ in the other factors of eq. (85).

Similarly, we can hide the correlator $\langle U_A^\dagger(\mathbf{k}_{2\perp})U(\mathbf{k}'_{2\perp}) \rangle_{aa'}$ in a function φ_A that describes the nucleus. By analogy with eq. (87), we define it as follows:

$$\begin{aligned} \langle U^\dagger(\mathbf{k}_{2\perp})U(\mathbf{k}'_{2\perp}) \rangle_{aa'} &= \frac{g^2 N \delta_{aa'}}{\pi d_A} \frac{1}{k_{2\perp}^2} \\ &\times \int d^2 \mathbf{Y}_\perp e^{i(\mathbf{k}'_{2\perp} - \mathbf{k}_{2\perp}) \cdot \mathbf{Y}_\perp} \frac{d\varphi_A(\mathbf{k}_{2\perp} | \mathbf{Y}_\perp - \mathbf{b})}{d^2 \mathbf{Y}_\perp}, \end{aligned} \quad (88)$$

where \mathbf{b} is the impact parameter of the collision. The normalization of φ_A has been chosen so that it is consistent with eq. (87) in the case of a dilute target. It is important to note that the function φ_A is not the canonical unintegrated gluon distribution of the nucleus, i.e. the expectation value of the number operator $a_k^\dagger a_k$: it only coincides with the unintegrated gluon distribution at large \mathbf{k}_\perp . The correct interpretation of the function φ_A is that it is the square of the scattering amplitude of a gluon on the target nucleus.

Neglecting the difference $\mathbf{k}_{1\perp} - \mathbf{k}'_{1\perp}$ everywhere except in the exponentials, and using the explicit expression of C_U^2 , we obtain:

$$\overline{N}_g = \frac{16\alpha_s N}{\pi d_A q_\perp^2} \int \frac{d^3 \mathbf{q}}{(2\pi)^3 2E_q} \frac{d^2 \mathbf{k}_\perp}{(2\pi)^2} \int d^2 \mathbf{X}_\perp \frac{d\varphi_p(\mathbf{k}_\perp | \mathbf{X}_\perp)}{d^2 \mathbf{X}_\perp} \frac{d\varphi_A(\mathbf{q}_\perp - \mathbf{k}_\perp | \mathbf{X}_\perp - \mathbf{b})}{d^2 \mathbf{X}_\perp}. \quad (89)$$

This is the k_\perp -factorized form of the gluon multiplicity for pA collisions. We see that one can conveniently hide all the multiple scattering effects in a generalization of the definition of the unintegrated gluon distribution of the nucleus, the hard (perturbative) part of the matrix element remaining the same as in pp collisions.

This expression for proton-nucleus collisions was first derived by Kovchegov and Mueller [35], though not expressed in this form (see also Kopeliovich et al. [51] and Braun [46]). It was re-written in this form first by Kovchegov and Tuchin for deeply inelastic scattering [44] and subsequently by Kharzeev, Kovchegov and Tuchin for the pA case [45].

4.2 Comparison with Dumitru and McLerran

In this section, we compare our result for gluon production with the result obtained by Dumitru and McLerran [43] in the Fock-Schwinger gauge ($x^+ A^- + x^- A^+ = 0$) which is an interpolation between two light-cone gauges. It is simpler to do this comparison at the level of the formula given by eq. (85). The latter may be rewritten as

$$\begin{aligned} \frac{d\overline{N}_g}{d^2 \mathbf{q}_\perp dy} &= -\frac{1}{16\pi^3} \int \frac{d^2 \mathbf{k}_{1\perp}}{(2\pi)^2} \frac{d^2 \mathbf{k}'_{1\perp}}{(2\pi)^2} \frac{C_U(q, \mathbf{k}_{1\perp}) \cdot C_U(q, \mathbf{k}'_{1\perp})}{k_{1\perp}^2 k'_{1\perp}{}^2} \\ &\times \langle \rho_{p,a}^\dagger(\mathbf{k}_{1\perp}) \rho_{p,a'}(\mathbf{k}'_{1\perp}) \rangle \langle U^\dagger(\mathbf{k}_{2\perp}) U(\mathbf{k}'_{2\perp}) \rangle_{aa'}. \end{aligned} \quad (90)$$

In the paper by Dumitru and McLerran, the gluon spectrum is given by

$$\frac{d\bar{N}_g}{d^2\mathbf{q}_\perp dy} \Big|_{D-ML} = \frac{2}{(2\pi)^2} \text{tr}_c \langle |a_1|^2 + |a_2|^2 \rangle, \quad (91)$$

with coefficients a_1 and a_2 (converted to our notations) defined to be

$$\begin{aligned} a_1(\mathbf{q}_\perp) &= \frac{e^{3i\pi/4}}{\sqrt{\pi}q_\perp} \int d^2\mathbf{x}_\perp e^{-i\mathbf{k}_\perp \cdot \mathbf{x}_\perp} \delta^{ij} \alpha_1^{ai}(\mathbf{x}_\perp) \partial_x^j \left(t^b U(\mathbf{x}_\perp)_{ba} \right), \\ a_2(\mathbf{q}_\perp) &= \frac{e^{3i\pi/4}}{\sqrt{\pi}q_\perp} \int d^2\mathbf{x}_\perp e^{-i\mathbf{k}_\perp \cdot \mathbf{x}_\perp} \epsilon^{ij} \partial_x^j \left(\alpha_1^{ai}(\mathbf{x}_\perp) t^b U(\mathbf{x}_\perp)_{ba} \right). \end{aligned} \quad (92)$$

t^b is a generator of the fundamental representation of $SU(N)$ and tr_c denotes a trace of color matrices. In these equations, $\alpha_1^{ai}(\mathbf{x}_\perp)$ is defined by the relation

$$\alpha_1^{ai}(\mathbf{x}_\perp) \equiv -\frac{\partial_x^i}{\nabla_\perp^2} \rho_{p,a}(\mathbf{x}_\perp). \quad (93)$$

It is convenient to replace $U(\mathbf{x}_\perp)$ and $\alpha_1^{ai}(\mathbf{x}_\perp)$ by their Fourier transforms in the expressions for a_1 and a_2 :

$$\begin{aligned} U(\mathbf{x}_\perp) &= \int \frac{d^2\mathbf{k}_{2\perp}}{(2\pi)^2} e^{i\mathbf{k}_{2\perp} \cdot \mathbf{x}_\perp} U(\mathbf{k}_{2\perp}), \\ \alpha_1^{ai}(\mathbf{x}_\perp) &= \int \frac{d^2\mathbf{k}_{1\perp}}{(2\pi)^2} e^{i\mathbf{k}_{1\perp} \cdot \mathbf{x}_\perp} \frac{ik_{1\perp}^i}{k_{1\perp}^2} \rho_{p,a}(\mathbf{k}_{1\perp}). \end{aligned} \quad (94)$$

We can thus write a_1 and a_2 as

$$\begin{aligned} a_1(\mathbf{q}_\perp) &= \frac{e^{3i\pi/4}}{\sqrt{\pi}q_\perp} \int \frac{d^2\mathbf{k}_{1\perp}}{(2\pi)^2} \delta^{ij} \frac{k_1^i k_2^j}{k_{1\perp}^2} \rho_{p,a}(\mathbf{k}_{1\perp}) t^b U(\mathbf{k}_{2\perp})_{ba}, \\ a_2(\mathbf{q}_\perp) &= \frac{e^{3i\pi/4}}{\sqrt{\pi}q_\perp} \int \frac{d^2\mathbf{k}_{1\perp}}{(2\pi)^2} \epsilon^{ij} \frac{k_1^i k_2^j}{k_{1\perp}^2} \rho_{p,a}(\mathbf{k}_{1\perp}) t^b U(\mathbf{k}_{2\perp})_{ba}, \end{aligned} \quad (95)$$

where now we have implicitly $\mathbf{k}_{2\perp} = \mathbf{q}_\perp - \mathbf{k}_{1\perp}$. Squaring these coefficients, taking the trace of their sum, averaging over the sources and inserting the result in eq. (91), we obtain:

$$\begin{aligned} \frac{d\bar{N}_g}{d^2\mathbf{q}_\perp dy} \Big|_{D-ML} &= \frac{1}{4\pi^3 q_\perp^2} \int \frac{d^2\mathbf{k}_{1\perp}}{(2\pi)^2} \frac{d^2\mathbf{k}'_{1\perp}}{(2\pi)^2} \frac{[\delta^{ij} \delta^{kl} + \epsilon^{ij} \epsilon^{kl}] k_1^i k_2^j k_1'^k k_2'^l}{k_{1\perp}^2 k_{1\perp}'^2} \\ &\quad \times \langle \rho_{p,a}^\dagger(\mathbf{k}_{1\perp}) \rho_{p,a'}(\mathbf{k}'_{1\perp}) \rangle \langle U^\dagger(\mathbf{k}_{2\perp}) U(\mathbf{k}'_{2\perp}) \rangle_{aa'}. \end{aligned} \quad (96)$$

At this point, it is trivial (although a bit tedious) to verify the identity

$$-C_U(q, \mathbf{k}_{1\perp}) \cdot C_U(q, \mathbf{k}'_{1\perp}) = \frac{4}{q_\perp^2} [\delta^{ij} \delta^{kl} + \epsilon^{ij} \epsilon^{kl}] k_1^i k_2^j k_1'^k k_2'^l, \quad (97)$$

if the vector q is on-shell and $k_1 + k_2 = k'_1 + k'_2 = q$. This ends the proof that our result is equivalent to the result obtained by Dumitru and McLerran. *Note that this equivalence works regardless of the model one chooses for the functional average over the hard sources. One need not specify this average to prove our result, nor even assume translational invariance in the transverse plane.*

5 Cronin effect in classical gluon production

The Cronin effect was discovered in proton-nucleus collisions in the late 70's [62–64]. The effect observed was a hardening of the transverse momentum spectrum in proton-nucleus collisions, relative to proton-proton collisions, that sets in at transverse momenta of order $k_{\perp} \sim 1 - 2$ GeV, and disappears at much larger k_{\perp} 's. A corresponding depletion was seen at low transverse momenta, accompanied by a softening of the spectrum. At that time, and indeed subsequently, the effect was interpreted as arising from the multiple scatterings of partons from the proton off partons from the nucleus [65]. As a result of such scatterings, the partons acquire a transverse momentum kick, shifting their momenta from lower to higher values, hereby causing the observed respective depletion and enhancement. At high k_{\perp} , the higher twist effects, which, in the language of perturbative QCD, are responsible for multiple scattering [66,67] are suppressed by powers of k_{\perp} . The relative enhancement of the cross-sections at moderate k_{\perp} 's should thus die away – and indeed, the data seemed to suggest as much. Though a qualitative understanding of the previously observed Cronin effect was suggested by perturbative QCD, a quantitative agreement for all its features (such as, for instance, the flavor dependence) is still lacking.

The high energy deuteron-nucleus collisions at RHIC (and at the LHC in the near future) add another dimension to the Cronin effect, namely, its energy dependence. At high collision energies, the projectile probes the small x partons in the nuclear wave-function, whose distribution may be modified by the nuclear medium. As the energy increases, there are effectively more of them to scatter from and this should lead to an enhancement of the effect at higher energies. Eventually, the number of gluons saturates, implying a corresponding saturation of the effect of multiple scatterings. However, what happens also at high energies is a change in the spectrum and, as we shall see, that modifies qualitatively the net effect of the multiple scatterings. These various types of behaviors will be illustrated in this section.

First data from RHIC provide indications on how the Cronin effect is modified with energy or, equivalently, with the rapidity. The x values probed in these experiments, at $k_{\perp} \sim 2$ GeV, range from 10^{-2} in the central rapidity region down to 10^{-4} at very forward rapidities. The most dramatic result is that of the BRAHMS experiment [1] which has taken data up to pseudo-rapidities $\eta = 3.2$ ¹⁵. It is observed that the Cronin peak shrinks rapidly with rapidity and at higher rapidity, one sees that there is a significant suppression instead. Equally interesting is the centrality dependence of the effect [1]. At central rapidities, one observes that the Cronin peak is enhanced in more central collisions, while, for forward rapidities, the trend is reversed: more central collisions at forward rapidities show a greater suppression than peripheral collisions!

The Cronin effect has been studied in the Color Glass Condensate frame-

¹⁵The trends seen by BRAHMS are also corroborated by PHOBOS, PHENIX and STAR in more limited kinematic ranges [2–4]. One can expect in the near future results from more detailed studies of the forward region in Deuteron-Gold collisions at RHIC from all experiments-in particular from STAR and PHENIX.

work by a number of authors. These studies range from semi-quantitative [47, 48, 50, 52–54] to detailed numerical solutions of the Balitsky-Kovchegov equation [55]. There is a consensus among all these authors that the Cronin effect is suppressed at forward rapidities. It was shown early on by Dumitru, Jalilian-Marian, and one of us [47, 48, 50] that the McLerran-Venugopalan model shows a greater Cronin enhancement for larger values of the saturation scale Q_s . In particular, the location and the width of the Cronin peak are roughly proportional to Q_s . The saturation scale can be larger for greater centralities or for smaller values of x . The model therefore correctly predicts the greater enhancement for more central collisions for $\eta = 0$ at RHIC. However, it fails badly when one goes to forward rapidities. Because x is small, the saturation scale Q_s is larger and one gets more enhancement – rather than the observed suppression. One possible cause for the failure of the McLerran-Venugopalan model is that it does not include the quantum evolution of the parton distributions. In fact, it was noticed early on that quantum corrections to the McLerran-Venugopalan model are large [68, 69]. The proper treatment of these corrections was performed by several authors – known collectively by their acronyms as JIMWLK [15–27], leading to the evolution equation for the weight functional $W_A[x_0^A, \rho_A]$ for the sources ρ_A . This equation can equivalently be re-expressed as an infinite hierarchy of ordinary differential equations for n -point correlators: $\langle UU \rangle$, $\langle UUU \rangle$, $\langle UUU \dots \rangle$, where U is a Wilson line¹⁶ in the background field created by the source ρ_A . For the 2-point function $\langle UU^\dagger \rangle$, a closed equation exists in the large N limit: it is the Balitsky-Kovchegov equation [21, 23]. This equation reduces to the well-known BFKL equation in the low density or large transverse momentum limit. Both the BK equation and the JIMWLK equation have been studied in analytical approximations (see [70] and [26] respectively). The BK equation has been studied numerically [71, 72] and has been applied to a recent study of the Cronin effect [55]. The JIMWLK equation has been studied analytically in the “super saturated” small x region [73]. Detailed numerical solutions have only become available recently [74].

In this section, we will discuss the different features of the Cronin effect in the Color Glass Condensate framework. In all cases studied, the weight functional is a Gaussian. Then, the Cronin effect can be equivalently understood in terms of independent multiple scatterings, and the explicit connection between the present formalism and Glauber’s formalism of multiple scatterings is recalled in appendix C. We will first consider in detail the classical (no quantum evolution) McLerran-Venugopalan model’s predictions for the Cronin effect. We next include quantum evolution “naively” by introducing “by hand” an x dependence in the saturation scale: $Q_s \rightarrow Q_s(x)$, along the lines first suggested by Golec-Biernat and Wüsthoff based on their parameterizations of the HERA small- x data [75, 76]. We show that this gives the wrong behavior for the Cronin effect at forward rapidities. We next consider analytical mean-field solutions of the JIMWLK equation – in a saturated regime where the system has no memory of its initial conditions at small x . It was shown by Iancu, Itakura and

¹⁶For more details, see [28–30].

McLerran [73], that the weight functional of the sources in this regime is also a Gaussian, albeit a non-local Gaussian distribution. This Gaussian solution can be incorporated in our study of the Cronin effect, and we find that if one is in this “super saturated” regime already at $y = 0$, the Cronin effect is suppressed. Further evolution to $y = 3$ increases the suppression, but not by a great deal. We will discuss the implications of this study at the end of this section.

5.1 Plain MV model

If we consider a large nucleus, there is an approximate translation invariance of the correlator $\langle UU^\dagger \rangle$, which implies that the function $d\varphi_A/d^2\mathbf{X}_\perp$ is approximately independent of the location \mathbf{X}_\perp in the transverse plane:

$$\frac{d\varphi_A(\mathbf{k}_\perp|\mathbf{X}_\perp)}{d^2\mathbf{X}_\perp} = \frac{\pi^2 d_A}{4Ng^2} k_\perp^2 C(k_\perp), \quad (98)$$

where we denote:

$$\int d^2\mathbf{r}_\perp e^{i\mathbf{k}_\perp \cdot \mathbf{x}_\perp} \langle U^\dagger(0)U(\mathbf{x}_\perp) \rangle_{ab} \equiv C(k_\perp)\delta_{ab}. \quad (99)$$

This object is identical to the quantity $C(k_\perp)$ introduced in a paper by one of us and Peshier [49,77], except that it is now a correlator of Wilson lines in the adjoint representation. (This quantity, again for fundamental Wilson lines, was also studied in [14,78] where it was denoted $\gamma(k_\perp)$.) In the MV model, where the functional W_A is a Gaussian weight given by

$$W_A[\rho_A] \equiv \exp \left[- \int d^2\mathbf{x}_\perp \frac{\rho_{A,a}(\mathbf{x}_\perp)\rho_{A,a}(\mathbf{x}_\perp)}{2\mu_A^2} \right], \quad (100)$$

this correlator can be computed in closed form. We get:

$$\langle U^\dagger(0)U(\mathbf{x}_\perp) \rangle_{ab} = \delta_{ab} \exp \left[- \frac{g^4 N \mu_A^2}{2} \int d^2\mathbf{y}_\perp [G_0(\mathbf{y}_\perp) - G_0(\mathbf{y}_\perp - \mathbf{x}_\perp)]^2 \right], \quad (101)$$

where G_0 is the 2-dimensional massless propagator:

$$G_0(\mathbf{x}_\perp - \mathbf{y}_\perp) \equiv \int \frac{d^2\mathbf{k}_\perp}{(2\pi)^2} \frac{e^{i\mathbf{k}_\perp \cdot (\mathbf{x}_\perp - \mathbf{y}_\perp)}}{k_\perp^2}. \quad (102)$$

In terms of the function C , the gluon spectrum reads:

$$\frac{d\bar{N}_g}{d^2\mathbf{q}_\perp dy} = \frac{1}{16\pi^3 q_\perp^2} \int \frac{d^2\mathbf{k}_\perp}{(2\pi)^2} k_\perp^2 C(\mathbf{k}_\perp) \varphi_p(\mathbf{q}_\perp - \mathbf{k}_\perp). \quad (103)$$

At large transverse momentum k_\perp , we have the following behavior for $C(k_\perp)$:

$$k_\perp^2 C(k_\perp) \approx \frac{g^4 N \mu_A^2}{k_\perp^2}, \quad (104)$$

which is the standard bremsstrahlung perturbative tail. Note that this tail is proportional to $\mu_A^2 \propto A^{1/3}$, where A is the atomic number of the nucleus. However, at lower transverse momentum (k_\perp^2 of the order of $Q_{s,A}^2 \sim g^4 N \mu_A^2$ or smaller), the $1/k_\perp^2$ growth stops and the function $k_\perp^2 C(k_\perp)$ remains bounded when $k_\perp \rightarrow 0$. This function was evaluated numerically in [49] and the typical

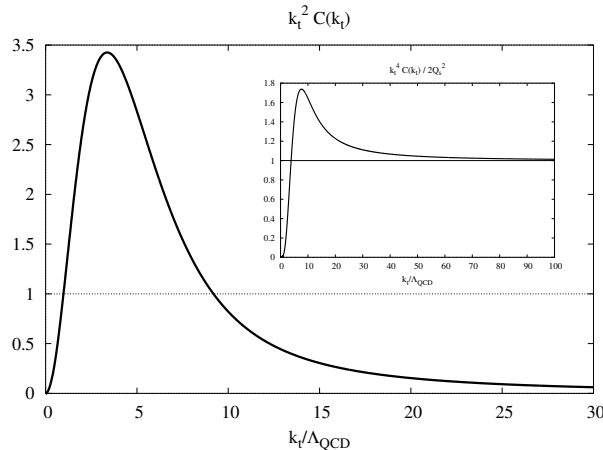


Figure 7: Behavior of $\varphi(k_\perp) \propto k_\perp^2 C(k_\perp)$ in the McLerran-Venugopalan model. In the upper right corner is plotted the quantity $k_\perp^4 C(k_\perp)$, which shows that the tail of the function $\varphi(k_\perp)$ behaves like $1/k_\perp^2$. In this plot, we have taken $Q_{s,A}^2 \equiv g^4 N \mu_A^2 / 2 = 25 \Lambda_{QCD}^2$, where Λ_{QCD} is the infrared cutoff (which sets the momentum scale).

behavior of $k_\perp^2 C(k_\perp)$ is illustrated in figure 7.

At low collision energy, we don't really know what the proton unintegrated gluon distribution is because it is mostly a non-perturbative quantity. In order to perform a quick numerical study of eq. (103), we take the proton unintegrated gluon distribution $\varphi_p(k_\perp)$ to be proportional¹⁷ to $k_\perp^2 C(k_\perp)$, with the same function $C(k_\perp)$ but now evaluated with a much smaller density μ_p^2 (or saturation scale $Q_{s,p}^2$). We have now a $C_A(k_\perp)$ and a $C_p(k_\perp)$, corresponding respectively to μ_A^2 and μ_p^2 , and the ratio of the two saturation scales is taken to be:

$$\frac{\mu_A^2}{\mu_p^2} = A^{1/3} \approx 6. \quad (105)$$

¹⁷Obviously, using a proton gluon distribution proportional to $k_\perp^2 C(k_\perp)$, i.e. to a correlator of Wilson lines, is a totally unjustified ansatz. Indeed, we have only proven k_\perp -factorization for a calculation performed at the lowest order in the source describing the proton. However, this ansatz for φ_p has the expected large k_\perp tail, and here one could simply see it as a way of introducing an infrared cutoff (necessary because the bremsstrahlung spectrum in $1/k_\perp^2$ is not integrable at low k_\perp). Moreover, what we take for φ_p is not essential for the discussion of the Cronin effect, as it is mostly due to properties of the small- x wave function of the target.

Up to a constant normalization factor, we have

$$\left. \frac{d\bar{N}_g}{d^2\mathbf{q}_\perp dy} \right|_{pA} \propto \frac{1}{q_\perp^2} \int \frac{d^2\mathbf{k}_\perp}{(2\pi)^2} (\mathbf{q}_\perp - \mathbf{k}_\perp)^2 k_\perp^2 C_A(\mathbf{k}_\perp) C_p(\mathbf{q}_\perp - \mathbf{k}_\perp), \quad (106)$$

for proton-nucleus collisions, and

$$\left. \frac{d\bar{N}_g}{d^2\mathbf{q}_\perp dy} \right|_{pp} \propto \frac{1}{q_\perp^2} \int \frac{d^2\mathbf{k}_\perp}{(2\pi)^2} (\mathbf{q}_\perp - \mathbf{k}_\perp)^2 k_\perp^2 C_p(\mathbf{k}_\perp) C_p(\mathbf{q}_\perp - \mathbf{k}_\perp), \quad (107)$$

for pp collisions. The spectrum in pA collisions can be estimated numerically using eq. (106), and we have displayed the result in figure 8. One can see clearly

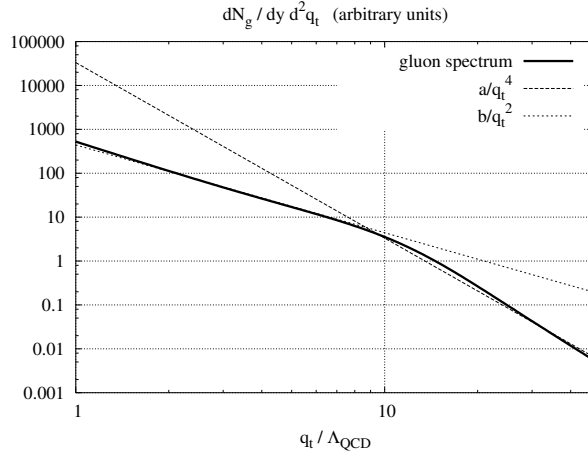


Figure 8: Numerical calculation of the spectrum in pA collisions. We use $Q_{s,A}/\Lambda_{QCD} = 5$ and $Q_{s,p}/\Lambda_{QCD} = 2$. The dotted curves are fits to power laws.

on this plot a change of behavior between a tail in $1/q_\perp^4$ and an intermediate region where the slope of the spectrum is $1/q_\perp^2$, as predicted by Dumitru and McLerran.

We can also estimate the “nuclear enhancement ratio” R_{pA} as follows:

$$R_{pA} \equiv \frac{\frac{1}{N_{\text{coll}}} \left. \frac{d\bar{N}_g}{d^2\mathbf{q}_\perp dy} \right|_{pA}}{\left. \frac{d\bar{N}_g}{d^2\mathbf{q}_\perp dy} \right|_{pp}} = \frac{1}{A^{1/3}} \frac{\int \frac{d^2\mathbf{k}_\perp}{(2\pi)^2} (\mathbf{q}_\perp - \mathbf{k}_\perp)^2 k_\perp^2 C_A(\mathbf{q}_\perp - \mathbf{k}_\perp) C_p(\mathbf{k}_\perp)}{\int \frac{d^2\mathbf{k}_\perp}{(2\pi)^2} (\mathbf{q}_\perp - \mathbf{k}_\perp)^2 k_\perp^2 C_p(\mathbf{q}_\perp - \mathbf{k}_\perp) C_p(\mathbf{k}_\perp)}. \quad (108)$$

We have computed numerically the ratio of these integrals, and the result is plotted in figure 9. One can see clearly the Cronin effect as a small bump at $q_\perp/\Lambda_{QCD} \approx 11$: the ratio is smaller than unity at small momenta, and then remains larger than 1 at larger momenta.

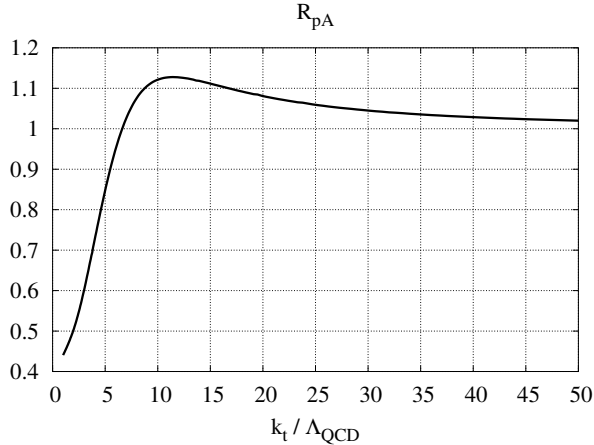


Figure 9: The ratio R_{pA} in the McLerran-Venugopalan model, without quantum evolution. We use the values $Q_{s,A}/\Lambda_{QCD} = 4.9$ and $Q_{s,p}/\Lambda_{QCD} = 2$, which corresponds to a ratio $\mu_A^2/\mu_p^2 \approx 6$.

When the saturation scale of the nucleus is much larger than that of the proton, the location of the Cronin peak can be estimated in a semi-quantitative way as follows. A good approximation of the behavior of the function $C_A(k_{\perp})$ for transverse momenta k_{\perp} comparable to the saturation scale or smaller is:

$$C_A(k_{\perp}) \approx \frac{8\pi^2}{Q_{s,A}^2} e^{-2\pi k_{\perp}^2 / \bar{Q}_{s,A}^2}, \quad (109)$$

with $\bar{Q}_{s,A}^2 \equiv Q_{s,A}^2 \ln(Q_{s,A}^2 / \Lambda_{QCD}^2)$ and $Q_{s,A}^2 \equiv 8\pi^2 \alpha_s^2 N \mu_A^2$. Assuming that the ratio R_{pA} can be approximated by the ratio of the distributions in the targets¹⁸

$$R_{pA} \approx \frac{C_A(k_{\perp})}{A^{1/3} C_p(k_{\perp})}, \quad (110)$$

and that $C_p(k_{\perp}) \propto 1/k_{\perp}^4$ in the relevant region¹⁹, we see that R_{pA} has a maximum at $k_{\perp} = \bar{Q}_{s,A} / \sqrt{\pi}$. The apparent mismatch with the location of the maximum in figure 9 is due to an insufficient separation between $Q_{s,A}$ and $Q_{s,p}$ (in addition to the fact that the two saturation scales are not very large compared to Λ_{QCD}).

¹⁸This would be exact if the unintegrated gluon distribution of the projectile were proportional to a $\delta(\mathbf{k}_{\perp})$. In practice, this is a reasonable approximation if the saturation scale in the nucleus target is much larger than that of the projectile.

¹⁹In the regime where the saturation scale in the proton is much smaller than that in the nucleus, the bulk of the gluon distribution of the nucleus corresponds to momenta that are in the tail of the gluon distribution of the proton.

5.2 Quantum evolution introduced via $\mu_A^2(x)$

The results of the previous subsection have been obtained in the plain McLerran-Venugopalan model, which does not contain any quantum evolution. This means that the quantities μ_A^2, μ_p^2 (i.e. the saturation scales of the nucleus and of the proton) do not depend on the momentum fraction x . One consequence is that the gluon multiplicity is exactly boost invariant – independent of y . A naive extension of the previous calculations is to assume that the only effect of quantum evolution is to change the values of μ_A^2 and μ_p^2 by making them x dependent, while preserving the local Gaussian nature of the functional weight. Following a popular parameterization, originally due to Golec-Biernat and Wüsthoff [75,76], we parametrize the saturation scale as

$$\begin{aligned} Q_{s,p}^2/Q_0^2 &= \left(\frac{x_0}{x}\right)^\lambda, \\ Q_{s,A}^2/Q_0^2 &= A^{1/3} \left(\frac{x_0}{x}\right)^\lambda, \end{aligned} \quad (111)$$

with $Q_0 \equiv 1$ GeV. We use the values of x_0 and λ obtained in the recent paper by Iancu, Itakura and Munier: $x_0 = 0.67 \cdot 10^{-4}$ and $\lambda = 0.25$ from their fits to the HERA F_2 data [79]. The values of x in the proton and in the nucleus are given by:

$$\begin{aligned} x_p &= \frac{q_\perp}{\sqrt{s}} e^{+y}, \\ x_A &= \frac{q_\perp}{\sqrt{s}} e^{-y}, \end{aligned} \quad (112)$$

where $\sqrt{s} = 200$ GeV is the energy per nucleon in the collision. For definiteness, we set the infrared cutoff to $\Lambda_{QCD} = 200$ MeV. We then simply repeat the previous calculation with the following formula for R_{pA} :

$$R_{pA} = \frac{1}{A^{1/3}} \frac{\int \frac{d^2\mathbf{k}_\perp}{(2\pi)^2} (\mathbf{q}_\perp - \mathbf{k}_\perp)^2 k_\perp^2 C_A(x_A, \mathbf{k}_\perp) C_p(x_p, \mathbf{q}_\perp - \mathbf{k}_\perp)}{\int \frac{d^2\mathbf{k}_\perp}{(2\pi)^2} (\mathbf{q}_\perp - \mathbf{k}_\perp)^2 k_\perp^2 C_p(x_A, \mathbf{k}_\perp) C_p(x_p, \mathbf{q}_\perp - \mathbf{k}_\perp)}. \quad (113)$$

The results of the numerical evaluation of this ratio are displayed in figure 10.

The characteristic Cronin bump is still present both at $y = 0$ and at $y = 3$. The primary difference is that at larger rapidity the maximum is more pronounced and is pushed towards larger momenta. This is a consequence of the fact that it is the Q_s of the nucleus that determines the location of the maximum to a large extent (see eqs. (109) and (110)). Similarly, more central collisions would give a greater enhancement as well, since they correspond to a larger Q_s . This picture is consistent with the centrality dependence observed at $y = 0$ in Deuteron-Gold collisions at RHIC. It is however in complete disagreement, at forward rapidities, with the observation made recently by the BRAHMS experiment [1].

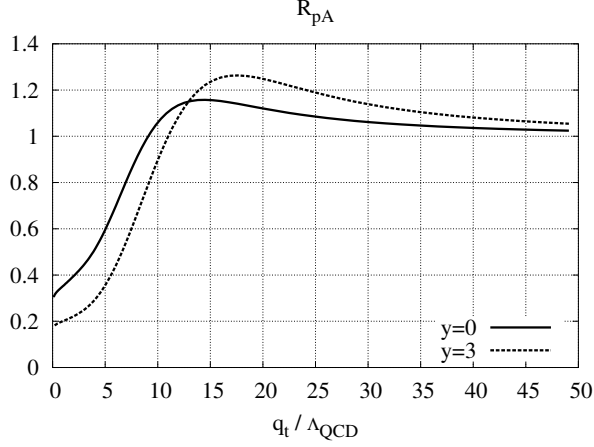


Figure 10: The ratio R_{pA} in the McLerran-Venugopalan model, with quantum evolution introduced via the x dependence of the saturation scale.

5.3 Non-local Gaussian distribution

One can generalize the previous model for the correlator $\langle U^\dagger(0)U(\mathbf{x}_\perp) \rangle_{ab}$ by allowing transverse non-localities in the Gaussian functional W_A . This amounts to generalizing eq. (100) by allowing μ_A^2 to depend not only on x but also on the transverse coordinates:

$$W_A[x, \rho_A] \equiv \exp \left[- \int d^2 \mathbf{x}_\perp d^2 \mathbf{y}_\perp \frac{\rho_{A,a}(\mathbf{x}_\perp) \rho_{A,a}(\mathbf{y}_\perp)}{2\mu_A^2(x, \mathbf{x}_\perp - \mathbf{y}_\perp)} \right], \quad (114)$$

so that the average of a product of two ρ is given by

$$\langle \rho_{A,a}(\mathbf{x}_\perp) \rho_{A,b}(\mathbf{y}_\perp) \rangle = \delta_{ab} \mu_A^2(x, \mathbf{x}_\perp - \mathbf{y}_\perp). \quad (115)$$

In this model, we have assumed that the nucleus is invariant by translation in the transverse direction, which implies that μ_A^2 depends only on the difference $\mathbf{x}_\perp - \mathbf{y}_\perp$. For instance, this extension can be used to incorporate effects of color charge neutralization [80] by making the function $\mu_A^2(x, \mathbf{x}_\perp - \mathbf{y}_\perp)$ vanish at distances larger than a certain scale. In this model, one can still calculate in closed form the correlator of two Wilson lines:

$$\begin{aligned} \langle U^\dagger(0)U(\mathbf{x}_\perp) \rangle_{ab} &= \delta_{ab} \exp \left[- \frac{g^4 N}{2} \int d^2 \mathbf{y}_\perp d^2 \mathbf{z}_\perp \mu_A^2(x, \mathbf{y}_\perp - \mathbf{z}_\perp) \right. \\ &\quad \left. \times (G_0(\mathbf{y}_\perp) - G_0(\mathbf{y}_\perp - \mathbf{x}_\perp)) (G_0(\mathbf{z}_\perp) - G_0(\mathbf{z}_\perp - \mathbf{x}_\perp)) \right], \end{aligned} \quad (116)$$

or by going to Fourier space,

$$\langle U^\dagger(0)U(\mathbf{x}_\perp) \rangle_{ab} = \delta_{ab} \exp \left[-\frac{g^4 N}{2\pi} \int_0^{+\infty} \frac{dk_\perp}{k_\perp^3} (1 - J_0(k_\perp x_\perp)) \mu_A^2(x, k_\perp) \right], \quad (117)$$

with

$$\mu_A^2(x, k_\perp) \equiv \int d^2 \mathbf{x}_\perp e^{i\mathbf{k}_\perp \cdot \mathbf{x}_\perp} \mu_A^2(x, \mathbf{x}_\perp). \quad (118)$$

(We have assumed rotational invariance in the transverse plane. This Fourier transform therefore depends only on $k_\perp = |\mathbf{k}_\perp|$).

Such a non-local Gaussian distribution of color sources has in fact been predicted by Iancu, Itakura, McLerran [26], as a mean-field asymptotic solution of the JIMWLK evolution equation for the deeply saturated regime. In this asymptotic regime, the color neutralization is controlled by saturation physics and therefore happens at the scale Q_s instead of Λ_{QCD} , and the function μ^2 is given by:

$$\frac{g^4 N}{2\pi} \mu_A^2(x, k_\perp) \equiv \frac{2}{\gamma c} k_\perp^2 \ln \left(1 + \left(\frac{Q_{s,A}^2(x)}{k_\perp^2} \right)^\gamma \right). \quad (119)$$

In this equation, γ is some anomalous dimension ($\gamma \approx 0.64$ for BFKL) and $c \approx 4.84$. Before going on, it is instructive to discuss the unintegrated gluon distribution $\varphi(x, k_\perp) \propto k_\perp^2 C(x, k_\perp)$ for this model. The function $C(x, k_\perp)$ can be expanded in powers of $\mu_A^2(x, k_\perp)$, which corresponds to an expansion in the number of collisions (see the appendix C):

$$C(x, k_\perp) = C_1(x, k_\perp) + C_2(x, k_\perp) + \dots, \quad (120)$$

with²⁰

$$C_1(x, k_\perp) = g^4 N \frac{\mu_A^2(x, k_\perp)}{k_\perp^4} = \frac{4\pi}{\gamma c} \frac{1}{k_\perp^2} \ln \left(1 + \left(\frac{Q_{s,A}^2(x)}{k_\perp^2} \right)^\gamma \right), \quad (121)$$

and

$$C_2(x, k_\perp) = \frac{g^8 N^2}{2} \int \frac{d^2 \mathbf{p}_\perp}{(2\pi)^2} \left[\frac{\mu_A^2(x, p_\perp)}{p_\perp^4} \frac{\mu_A^2(x, |\mathbf{k}_\perp - \mathbf{p}_\perp|)}{(\mathbf{k}_\perp - \mathbf{p}_\perp)^4} - 2 \frac{\mu_A^2(x, k_\perp)}{k_\perp^4} \frac{\mu_A^2(x, p_\perp)}{p_\perp^4} \right]. \quad (122)$$

One can note that with the $\mu_A^2(x, p_\perp)$ given in eq. (119), this quantity is infrared finite. A numerical study of this 2-scattering correction shows that it is negative at low k_\perp and positive at large k_\perp . Therefore, the property that rescatterings move particles from low k_\perp to high k_\perp regions of the spectrum holds also in this model. However, since in this model the spectrum has a smaller slope at large k_\perp ($k_\perp^{-2(1+\gamma)}$ with $\gamma \approx 0.64$) than the MV model spectrum (k_\perp^{-4}), this effect of rescatterings is much less important. That higher

²⁰Note that $\varphi(x, k_\perp)$ depends on x and k_\perp only via the ratio $k_\perp/Q_s(x)$.

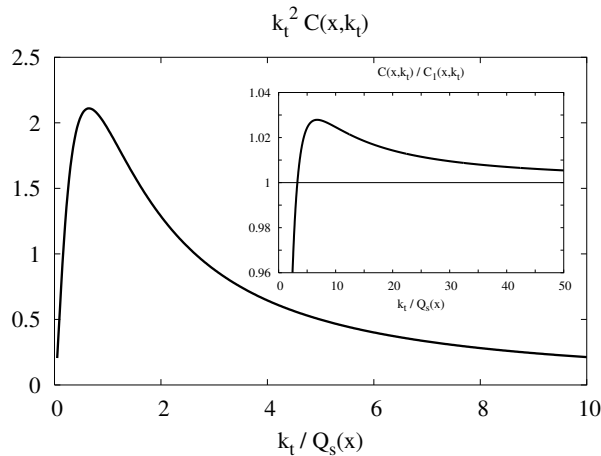


Figure 11: The function $k_{\perp}^2 C(x, k_{\perp})$ in the model defined by eq. (119) (plotted against $k_{\perp}/Q_{s,A}(x)$ thanks to its scaling properties). The insert in the upper right corner represents the ratio $C(x, k_{\perp})/C_1(x, k_{\perp})$.

twists tend to push the spectrum towards higher momenta is clearly seen in figure 11, where we have both represented the function $k_{\perp}^2 C(x, k_{\perp})$ (in the main plot), and the ratio $C(x, k_{\perp})/C_1(x, k_{\perp})$ (in the smaller insert). However, as the plot of $C(x, k_{\perp})/C_1(x, k_{\perp})$ also shows, the maximum over the single scattering term is now of only 3%, compared to 75% in the MV model (see the figure 7).

Assuming that the nuclear enhancement ratio R_{pA} is well approximated by eq. (110), we can obtain its asymptotic value at high k_{\perp} from the leading term $C_1(x, k_{\perp})$:

$$R_{pA} \underset{k_{\perp} \rightarrow \infty}{\approx} A^{-1/3} \left(\frac{Q_{s,A}^2}{Q_{s,p}^2} \right)^{\gamma} = A^{(\gamma-1)/3}. \quad (123)$$

Since $\gamma < 1$, this asymptotic value is smaller than 1. For $\gamma \approx 0.64$ and $A \approx 6$, we expect $R_{pA} \approx 0.52$ at large momentum (this ratio would probably go to 1 asymptotically if we let the anomalous dimension γ depend on transverse momentum and go to 1 at large momentum). Moreover, the ratio R_{pA} in this approximation is the ratio of two functions similar to the one plotted in the upper right corner of figure 11, rescaled horizontally by their respective Q_s and vertically by $Q_s^{2\gamma}$. Therefore, we expect the ratio R_{pA} to be below its asymptotic value $A^{(\gamma-1)/3}$ at small k_{\perp} , to eventually become larger than $A^{(\gamma-1)/3}$ and reach a very mild maximum (of a few percent), and finally to reach the asymptotic value from above.

We have studied the ratio R_{pA} numerically, and the results are displayed in the figure 12. The asymptotic value of R_{pA} is in relatively good agreement with the crude estimate given in eq. (123). It seems also that the very mild maximum we predicted on the basis of the approximate formula of eq. (110) has

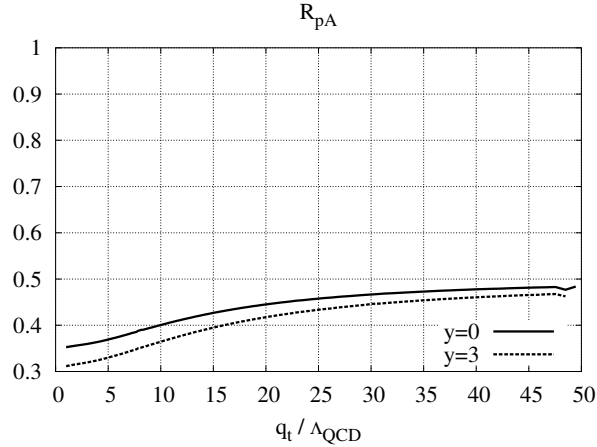


Figure 12: The ratio R_{pA} in the non-local Gaussian model of eq. (119).

been washed out by the convolution present in the exact formula. The shape of the curve now agrees qualitatively with BRAHMS data for $y = 3$. However, it also gives too much of a suppression at $y = 0$!

5.4 Interpretation of results

We can summarize the key results of the model calculations in this section as follows.

- Tree level partonic re-scattering responsible for the classical Cronin effect in high energy deuteron-Gold collisions is computable in the color glass condensate approach and when the weight for the color sources is Gaussian, the formalism reduces to the familiar Glauber formalism of independent multiple scatterings. In the simple McLerran-Venugopalan model, a peak appears at $k_{\perp} \sim Q_{s,A}$, which is more pronounced for more central collisions.
- Quantum corrections (due to small- x evolution) to the tree level partonic re-scattering can be “naively” included by letting $Q_s \rightarrow Q_s(x)$. The parameterization of $Q_s(x)$ as a function of x that we have used is of the form first suggested by Golec-Biernat and Wüsthoff but with the parameters from a recent fit by Iancu, Itakura and Munier to the HERA data. We call this model of quantum evolution naive because it does not consider the possibility that quantum evolution will change the form of the weight functional from the Gaussian form of the MV model. This naive quantum evolution model predicts a larger Cronin effect at larger rapidities (because Q_s grows as x decreases) and is in sharp disagreement with the RHIC d-Au data at forward rapidities [1].

- Proper quantum evolution in the CGC is described by the JIMWLK evolution equation. For the two-point correlator, of interest in Cronin studies, the large N limit is described by the Balitsky-Kovchegov equation. Like any other evolution equation, these equations evolve from an initial condition at some large $x = x_0$. At very small $x \ll x_0$, the system loses memory of its initial conditions. The JIMWLK equation, in this limit, is well described by a mean field approximation, and analytic expressions have been derived. Interestingly, the weight functional in this extreme limit is also a Gaussian, but with a non-local kernel. That is, the variance μ_A^2 of the Gaussian sources is now a function of k_\perp : $\mu_A^2(x) \rightarrow \mu_A^2(x, k_\perp)$. At low k_\perp , $\mu_A^2 \propto k_\perp^2 \ln(1 + (Q_s^2/k_\perp^2)^\gamma)$, where γ is an anomalous dimension ($\gamma \approx 0.64$ for BFKL evolution). Because the weight is Gaussian, the physics remains that of multiple independent scatterings. However, as our calculation in section 5.3 shows, the effects of multiple scatterings depend very much on the shape of the spectrum. It follows that the qualitative behavior of the ratio R_{pA} is different from what it is in the MV model with a local weight. If we assume that $y = 0$ and $y = 3$ at RHIC lie in this “super saturated” regime, we find a suppression both at $y = 0$ and $y = 3$. Thus while our results for $y = 3$ are qualitatively close to the BRAHMS data, the $y = 0$ results are decidedly not close to the corresponding $y = 0$ data. Our result therefore suggests that quantum evolution is not yet significant at $y = 0$. This of course was also evident from the disagreement of the prediction of Kharzeev, Levin and McLerran with the RHIC d-Au data at $y = 0$. Our result merely provides additional insight into why one has this disagreement.

From the comparison of the results of our simple studies with the qualitative features of the RHIC d-Au data emerges the following picture, which will have to be substantiated by more detailed (read quantitative) computations and a thorough confrontation to the experimental data. That the MV model works reasonably well at $x \sim 10^{-2}$ – central rapidities at RHIC – and reproduces key qualitative features of central d-Au collisions suggests that it has the right physics built in and that it could be a good model of the initial conditions for quantum evolution as a function of rapidity. The fact that at the same time the MV model fails badly at forward rapidities is suggestive of important (and non-trivial) quantum evolution effects that cannot be accounted for simply by a rescaling of the saturation momentum. This interpretation is consistent with the fact that the asymptotic mean-field solution of the JIMWLK evolution equation is in qualitative agreement with the d-Au data at $y = 3$. In particular, a prediction of this mean-field solution is that the ratio R_{pA} tends to $A^{(\gamma-1)/3}$ at large transverse momentum, where γ is the BFKL anomalous dimension. If there is some truth to this interpretation, one would also predict that the suppression of the ratio R_{pA} would change very little if even larger rapidities were available (since $y = 3$ seems to be already in the asymptotic regime). This corroborates the numerical results obtained previously from solutions of the BK equation by Albacete et al [55], and is also confirmed by Iancu, Itakura and

Triantafyllopoulos [81]. The preliminary RHIC d-Au data appear to similarly show a rapid change at lower rapidities but a weaker one at the higher rapidities probed.

6 Summary and Outlook

We have performed in this paper a systematic study of gluon production in pA collisions within the framework of the Color Glass Condensate. Working in the covariant gauge, we have solved the Yang-Mills equations to lowest order in the dilute proton source but to all orders in the nuclear source. Our explicit results for the gauge fields are useful in computing quark production in pA collisions. Our results on these are reported on in a companion paper. We have computed gluon production and demonstrated explicitly how k_{\perp} -factorization arises in this approach. We have demonstrated explicitly the equivalence of calculations of gluon production in different gauges.

The k_{\perp} -dependent distribution that describes the nucleus is proportional to a two-point correlator of Wilson lines. This suggests how small- x quantum evolution effects can be taken into account in studying proton-nucleus collisions in the CGC framework since the two point correlators satisfy non-linear evolution equations with x , or equivalently the rapidity y . We next studied in some detail the Cronin effect in the CGC framework. A rapid transition from the regime where multiple scattering effects are dominant to one where quantum evolution effects are dominant is suggested by simple analytical studies corroborating previous numerical studies. If confirmed by additional experimental results, this rapid transition has important ramifications in the near future for heavy ion experiments at the LHC and even for the proposed electron-heavy ion deeply inelastic scattering experiments (eRHIC) proposed at BNL.

Acknowledgements

R. V.'s research was supported by DOE Contract No. DE-AC02-98CH10886. We would like to thank I. Balitsky, E. Iancu, K. Itakura, J. Jalilian-Marian, K. Kajantie, Yu. Kovchegov, T. Lappi, S. Munier, D. Triantafyllopoulos, and K. Tuchin for useful discussions on this and related topics.

A Proof of equation (26)

Let's assume we want to solve the equation:

$$(\square_x + iF(x)\partial_x^+)A(x) = J(x), \quad (124)$$

with a source $J(x)$. The function $F(x)$ is some Hermitian matrix-valued object, and we assume that it does not depend on x^- , i.e. that it commutes with the derivative ∂_x^+ . We want to find the function $A(x)$ for times $x^+ > 0$, given

the value of $A(x^+ = 0, x^-, \mathbf{x}_\perp)$ (and maybe of its first derivatives, since the equation is of second order in derivatives) and the value of $A(x)$ and its first derivatives on the boundary of the “spatial” directions (here x^- and \mathbf{x}_\perp). In order to do that, we must start with the equations for $A(x)$ and for the free retarded propagator²¹:

$$\begin{aligned} (\overrightarrow{\square}_y + iF(y) \overrightarrow{\partial}_y^+) A(y) &= J(y), \\ G_R(x, y) (\overleftarrow{\square}_y - iF(y) \overleftarrow{\partial}_y^+) &= \delta(x - y). \end{aligned} \quad (125)$$

We have written the equation for the propagator with respect to its second point, which imposes to put the term $F(x)$ on the right because of its matrix nature. The arrows on the differential operators indicate on which side the derivatives act. Then, multiply the first equation by $G_R(x, y)$ (on the left), the second equation by $A(y)$ (on the right), subtract them, and integrate over y (with y^+ starting at 0). This gives:

$$\begin{aligned} A(x) &= \int_{y^+ > 0} d^4y G_R(x, y) J(y) \\ &+ \int_{y^+ > 0} d^4y \{ G_R(x, y) (\overleftarrow{\square}_y - iF(y) \overleftarrow{\partial}_y^+) A(y) \\ &\quad - G_R(x, y) (\overrightarrow{\square}_y + iF(y) \overrightarrow{\partial}_y^+) A(y) \}. \end{aligned} \quad (126)$$

This is a generalization to the case of eq. (124) of the standard Green’s theorem of electrostatics. The first term is the one we would naively expect if the initial and boundary conditions for the field and its derivative are zero. In order to deal with the second term, we first write $\square_y = 2\partial_y^+ \partial_y^- - \nabla_{y_\perp}^2$. For the term involving the transverse derivatives, we can write:

$$\begin{aligned} G_R(x, y) \overrightarrow{\nabla}_{y_\perp}^2 A(y) - G_R(x, y) \overleftarrow{\nabla}_{y_\perp}^2 A(y) \\ = \overrightarrow{\nabla}_{y_\perp} \cdot \left[G_R(x, y) \overrightarrow{\nabla}_{y_\perp} A(y) - G_R(x, y) \overleftarrow{\nabla}_{y_\perp} A(y) \right]. \end{aligned} \quad (127)$$

We then perform the integration over \mathbf{y}_\perp using Stokes theorem, and the corresponding term becomes:

$$\int_{y^+ > 0} dy^+ dy^- \oint_{\partial\mathbb{R}^2} d\mathbf{n}_\perp \cdot \left[G_R(x, y) \overrightarrow{\nabla}_{y_\perp} A(y) - G_R(x, y) \overleftarrow{\nabla}_{y_\perp} A(y) \right], \quad (128)$$

²¹The equation for the propagator when one acts on the right has been written by analogy with what happens when the “external field” is constant: in this case, the propagator is invariant by translation and depends only on $x - y$. Hence, the first derivatives with respect to y enter with the opposite sign compared to the first derivatives with respect to x , while the second derivatives are the same.

where $\partial\mathbb{R}^2$ is the boundary in the direction of transverse coordinates, and \mathbf{n}_\perp a unit normal vector on this boundary. Similarly, we can deal with the term in $\partial_y^+ \partial_y^-$ by first writing:

$$\begin{aligned} G_R(x, y) \overleftarrow{\partial}_y^+ \overleftarrow{\partial}_y^- A(y) - G_R(x, y) \overrightarrow{\partial}_y^+ \overrightarrow{\partial}_y^- A(y) \\ = \overrightarrow{\partial}_y^+ (G_R(x, y) \overleftarrow{\partial}_y^- A(y)) - \overrightarrow{\partial}_y^- (G_R(x, y) \overrightarrow{\partial}_y^+ A(y)). \end{aligned} \quad (129)$$

Therefore, the corresponding term gives:

$$\begin{aligned} 2 \int_{y^+ > 0} dy^+ d^2 \mathbf{y}_\perp \left[G_R(x, y) \overleftarrow{\partial}_y^- A(y) \right]_{y^- = -\infty}^{y^- = +\infty} \\ - 2 \int dy^- d^2 \mathbf{y}_\perp \left[G_R(x, y) \overrightarrow{\partial}_y^+ A(y) \right]_{y^+ = 0}^{y^+ = +\infty}. \end{aligned} \quad (130)$$

Using the fact that G_R is a retarded propagator, the boundary term at $y^+ = +\infty$ is zero. Finally, we need to deal with the term in $F(y) \partial_y^+$. We have:

$$\begin{aligned} -i \int_{y^+ > 0} d^4 y \{ G_R(x, y) F(y) \overleftarrow{\partial}_y^+ A(y) + G_R(x, y) F(y) \overrightarrow{\partial}_y^+ A(y) \} \\ = -i \int_{y^+ > 0} dy^+ d^2 \mathbf{y}_\perp [G_R(x, y) F(y) A(y)]_{y^- = -\infty}^{y^- = +\infty}. \end{aligned} \quad (131)$$

Here, we have used the fact that $F(y)$ commutes with ∂_y^+ and the fact that $G_R(x, y)$ is a retarded propagator. If we combine all the pieces together, we get:

$$\begin{aligned} A(x) &= \int_{y^+ > 0} d^4 y G_R(x, y) J(y) \\ &+ \int_{y^+ = 0} dy^- d^2 \mathbf{y}_\perp G_R(x, y) 2 \overrightarrow{\partial}_y^+ A(y) \\ &+ \int_{y^+ > 0} dy^+ dy^- \oint_{\partial\mathbb{R}^2} d\mathbf{n}_\perp \cdot \left[G_R(x, y) \overrightarrow{\nabla}_{y_\perp} A(y) - G_R(x, y) \overleftarrow{\nabla}_{y_\perp} A(y) \right] \\ &+ \int_{y^+ > 0} dy^+ d^2 \mathbf{y}_\perp \left[G_R(x, y) (2 \overleftarrow{\partial}_y^- - iF(y)) A(y) \right]_{y^- = -\infty}^{y^- = +\infty}. \end{aligned} \quad (132)$$

If we assume that the field and its derivatives vanish fast enough at infinity in the spatial directions, we get the simpler formula:

$$\begin{aligned} A(x) &= \int_{y^+ > 0} d^4 y G_R(x, y) J(y) \\ &+ \int_{y^+ = 0} dy^- d^2 \mathbf{y}_\perp G_R(x, y) 2 \overrightarrow{\partial}_y^+ A(y). \end{aligned} \quad (133)$$

Eq. (26) is a special case of this formula, where the source term J is zero. Naturally, in the above derivation, the hyperplane $y^+ = 0$ could have been replaced by any plane of constant y^+ on which we decide to set the initial condition.

B Simplification of equation (71)

In order to simplify eq. (71), we need to compute the following convolution product:

$$U \otimes (A_A^- \cdot T) \otimes V \equiv \int_0^\epsilon dx^+ U(\epsilon, x^+) (A_A^-(x^+) \cdot T) V(x^+, 0). \quad (134)$$

We have not written the transverse coordinates in this expression; they are the same for the three factors and are irrelevant for the following discussion. Let us first define

$$W(b^+, a^+ | x^+) \equiv \mathcal{P}_+ \left[\exp i \frac{g}{2} \int_{a^+}^{b^+} dz^+ (1 + \theta(z^+ - x^+)) A_A^-(z^+) \cdot T \right]. \quad (135)$$

This object interpolates between $U(b^+, a^+)$ and $V(b^+, a^+)$:

$$\begin{aligned} W(b^+, a^+ | x^+) &= V(b^+, a^+) \quad \text{if } x^+ \geq b^+, \\ W(b^+, a^+ | x^+) &= U(b^+, a^+) \quad \text{if } x^+ \leq a^+. \end{aligned} \quad (136)$$

We then have

$$\begin{aligned} \frac{\partial W(b^+, a^+ | x^+)}{\partial x^+} &= -i \frac{g}{2} W(b^+, x^+ | x^+) (A_A^-(x^+) \cdot T) W(x^+, a^+ | x^+) \\ &= -i \frac{g}{2} U(b^+, x^+) (A_A^-(x^+) \cdot T) V(x^+, a^+). \end{aligned} \quad (137)$$

Then, integrating over x^+ from 0 to ϵ , we get:

$$i \frac{g}{2} [U \otimes (A_A^- \cdot T) \otimes V] = U(\epsilon, 0) - V(\epsilon, 0). \quad (138)$$

Let us now go back to eq. (71). Using the fact that $0 \leq v^+ \leq \epsilon$, we can approximate $\exp(iq^- x^+) \approx 1$. Using eq. (138), we have at this point:

$$\begin{aligned} q^2 A^i(q) &= 2 \int dv^- d^2 \mathbf{v}_\perp e^{i(q^+ v^- - \mathbf{q}_\perp \cdot \mathbf{v}_\perp)} (V(\mathbf{v}_\perp) - U(\mathbf{v}_\perp)) \partial_v^i A_p^+(v) \\ &+ ig \int dv^- d^2 \mathbf{v}_\perp e^{i(q^+ v^- - \mathbf{q}_\perp \cdot \mathbf{v}_\perp)} \{ [U \otimes (\partial_v^i A_A^- \cdot T) \otimes V](\mathbf{v}_\perp) \\ &\quad - [U \otimes (A_A^- \cdot T) \otimes (\partial_v^i V)](\mathbf{v}_\perp) \} A_p^+(v). \end{aligned} \quad (139)$$

The next step is to make more explicit the derivative $\partial_v^i V$:

$$\partial_v^i V = i\frac{g}{2}[V \otimes (\partial_v^i A_A^- \cdot T) \otimes V], \quad (140)$$

which leads to²²:

$$\begin{aligned} & [U \otimes (\partial_v^i A_A^- \cdot T) \otimes V] - [U \otimes (A_A^- \cdot T) \otimes (\partial_v^i V)] \\ &= [U \otimes (\partial_v^i A_A^- \cdot T) \otimes V] - i\frac{g}{2}[U \otimes (A_A^- \cdot T) \otimes V \otimes (\partial_v^i A_A^- \cdot T) \otimes V] \\ &= i\frac{g}{2}[V \otimes (\partial_v^i A_A^- \cdot T) \otimes V] = \frac{2}{ig}\partial_v^i V. \end{aligned} \quad (143)$$

C Glauber interpretation of $C(k_\perp)$

It is fairly easy to write the Fourier transform $\delta_{ac}C(p_\perp)$ of $\langle U^\dagger(0)U(\mathbf{x}_\perp) \rangle$ in a form that makes its interpretation more intuitive in terms of the Glauber picture. Our starting point is eq. (117) (which is the most general form one can obtain in the case of a Gaussian distribution of ρ_A):

$$C(p_\perp) = \int d^2\mathbf{x}_\perp e^{i\mathbf{p}_\perp \cdot \mathbf{x}_\perp} \exp \left[-\frac{g^4 N}{2\pi} \int_0^{+\infty} \frac{dk_\perp}{k_\perp^3} (1 - J_0(k_\perp x_\perp)) \mu_A^2(x, k_\perp) \right]. \quad (144)$$

At this point, it is convenient to factor out of μ_A^2 a constant μ_0^2 that sets the scale:

$$\mu_A^2(x, k_\perp) \equiv \mu_0^2 f(x, k_\perp). \quad (145)$$

Typically, μ_0^2 is given by $\mu_0^2 = \rho L$, where ρ is the density in the target and L is the longitudinal size of the target. Then, we can introduce the following shorthands:

$$\begin{aligned} \sigma_{\text{tot}} &\equiv \frac{g^4 N}{2\pi} \int_0^{+\infty} \frac{dk_\perp}{k_\perp^3} f(x, k_\perp), \\ \sigma(\mathbf{x}_\perp) &\equiv \frac{g^4 N}{2\pi} \int_0^{+\infty} \frac{dk_\perp}{k_\perp^3} J_0(k_\perp x_\perp) f(x, k_\perp). \end{aligned} \quad (146)$$

²²We use the fact that the convolution product defined above is associative in the following sense:

$$[F \otimes A \otimes [G \otimes B \otimes H]] = [[F \otimes A \otimes G] \otimes B \otimes H]. \quad (141)$$

This can be proven simply by permuting the integrals over the two intermediate coordinates:

$$\int_0^\epsilon dx^+ \int_0^{x^+} dy^+ = \int_0^\epsilon dy^+ \int_{y^+}^\epsilon dx^+. \quad (142)$$

σ_{tot} is the total cross-section of an incoming parton on a parton of the target, and $\sigma(\mathbf{x}_\perp)$ is the Fourier transform of the differential cross-section (with respect to the transverse momentum transfer). We can therefore write:

$$\begin{aligned} C(p_\perp) &= e^{-\mu_0^2 \sigma_{\text{tot}}} \int d^2 \mathbf{x}_\perp e^{i \mathbf{p}_\perp \cdot \mathbf{x}_\perp} e^{\mu_0^2 \sigma(\mathbf{x}_\perp)} \\ &= e^{-\mu_0^2 \sigma_{\text{tot}}} \int d^2 \mathbf{x}_\perp e^{i \mathbf{p}_\perp \cdot \mathbf{x}_\perp} \sum_{n=0}^{+\infty} \frac{\mu_0^{2n}}{n!} [\sigma(\mathbf{x}_\perp)]^n . \end{aligned} \quad (147)$$

If we now replace each factor of $\sigma(\mathbf{x}_\perp)$ by its explicit expression as a Fourier transform of $\sigma(\mathbf{k}_\perp) \equiv g^4 N f(x, k_\perp) / k_\perp^4$, we get:

$$\begin{aligned} C(p_\perp) &= e^{-\mu_0^2 \sigma_{\text{tot}}} \sum_{n=0}^{+\infty} \frac{\mu_0^{2n}}{n!} \int \frac{d^2 \mathbf{k}_{1\perp}}{(2\pi)^2} \cdots \frac{d^2 \mathbf{k}_{n\perp}}{(2\pi)^2} \\ &\quad \times (2\pi)^2 \delta(\mathbf{k}_{1\perp} + \cdots + \mathbf{k}_{n\perp} - \mathbf{p}_\perp) \sigma(\mathbf{k}_{1\perp}) \cdots \sigma(\mathbf{k}_{n\perp}) . \end{aligned} \quad (148)$$

Finally, if we notice that:

$$\frac{\mu_0^{2n}}{n!} = \rho^n \int_0^L dz_1 \int_{z_1}^L dz_2 \cdots \int_{z_{n-1}}^L dz_n , \quad (149)$$

we see that the object $C(p_\perp)$ can be interpreted as the Glauber form of the cross-section of a parton undergoing multiple independent scatterings in the target (the index n in the sum is the number of such scatterings, and the z_i are the longitudinal coordinates of the scattering centers). Note that this correspondence is certainly only valid when the functional distribution of the source ρ_A is a Gaussian distribution (having a distribution with non-zero $\langle \rho_A \rho_A \rho_A \rangle$, $\langle \rho_A \rho_A \rho_A \rho_A \rangle \cdots$, introduces correlations between the different collisions and the Glauber picture of independent successive collisions breaks down). The form given in eq. (148) for $C(p_\perp)$ also makes obvious the following sum-rule:

$$\int \frac{d^2 \mathbf{p}_\perp}{(2\pi)^2} C(p_\perp) = 1 . \quad (150)$$

Indeed, integrating eq. (148) simply removes the delta function that was constraining the variables $\mathbf{k}_{i\perp}$, so that integrating over each $\mathbf{k}_{i\perp}$ now gives σ_{tot} . One can then re-exponentiate the sum over n , which gives a factor $\exp(\mu_0^2 \sigma_{\text{tot}})$ that compensates the prefactor $\exp(-\mu_0^2 \sigma_{\text{tot}})$.

References

- [1] R. Debbe, for the BRAHMS collaboration, talk given at QM2004, Oakland, USA, January 2004.

- [2] T. Frawley, for the PHENIX collaboration, talk given at QM2004, Oakland, January 2004.
- [3] P. Steinberg, for the PHOBOS collaboration, talk given at QM2004, Oakland, January 2004.
- [4] K. Schweda, for the STAR collaboration, talk given at QM2004, Oakland, January 2004.
- [5] A. Accardi, et al, CERN Yellow Report on “Hard Probes in Heavy Ion Collisions at the LHC: jet physics”, hep-ph/0310274.
- [6] A. Accardi, et al, CERN Yellow Report on “Hard Probes in Heavy Ion Collisions at the LHC: PDFs, shadowing and pA collisions”, hep-ph/0308248.
- [7] M. Bedjidian, et al, CERN Yellow Report on “Hard Probes in Heavy Ion Collisions at the LHC: heavy flavor physics”, hep-ph/0311048.
- [8] L.V. Gribov, E.M. Levin, M.G. Ryskin, Phys. Rept. **100**, 1 (1983).
- [9] A.H. Mueller, J-W. Qiu, Nucl. Phys. **B 268**, 427 (1986).
- [10] J.P. Blaizot, A.H. Mueller, Nucl. Phys. **B 289**, 847 (1987).
- [11] L.D. McLerran, R. Venugopalan, Phys. Rev. **D 49**, 2233 (1994).
- [12] L.D. McLerran, R. Venugopalan, Phys. Rev. **D 49**, 3352 (1994).
- [13] L.D. McLerran, R. Venugopalan, Phys. Rev. **D 50**, 2225 (1994).
- [14] L.D. McLerran, R. Venugopalan, Phys. Rev. **D 59**, 094002 (1999).
- [15] J. Jalilian-Marian, A. Kovner, A. Leonidov, H. Weigert, Nucl. Phys. **B 504**, 415 (1997).
- [16] J. Jalilian-Marian, A. Kovner, A. Leonidov, H. Weigert, Phys. Rev. **D 59**, 014014 (1999).
- [17] J. Jalilian-Marian, A. Kovner, A. Leonidov, H. Weigert, Phys. Rev. **D 59**, 034007 (1999).
- [18] J. Jalilian-Marian, A. Kovner, A. Leonidov, H. Weigert, Erratum. Phys. Rev. **D 59**, 099903 (1999).
- [19] A. Kovner, G. Milhano, Phys. Rev. **D 61**, 014012 (2000).
- [20] A. Kovner, G. Milhano, H. Weigert, Phys. Rev. **D 62**, 114005 (2000).
- [21] I. Balitsky, Nucl. Phys. **B 463**, 99 (1996).
- [22] Yu.V. Kovchegov, Phys. Rev. **D 54**, 5463 (1996).
- [23] Yu.V. Kovchegov, Phys. Rev. **D 61**, 074018 (2000).

- [24] J. Jalilian-Marian, A. Kovner, L.D. McLerran, H. Weigert, Phys. Rev. **D 55**, 5414 (1997).
- [25] E. Iancu, A. Leonidov, L.D. McLerran, Nucl. Phys. **A 692**, 583 (2001).
- [26] E. Iancu, A. Leonidov, L.D. McLerran, Phys. Lett. **B 510**, 133 (2001).
- [27] E. Ferreiro, E. Iancu, A. Leonidov, L.D. McLerran, Nucl. Phys. **A 703**, 489 (2002).
- [28] E. Iancu, R. Venugopalan, To be published in QGP3, Eds. R.C. Hwa and X.N.Wang, World Scientific, hep-ph/0303204.
- [29] E. Iancu, A. Leonidov, L.D. McLerran, Lectures given at Cargese Summer School on QCD Perspectives on Hot and Dense Matter, Cargese, France, 6-18 Aug 2001, hep-ph/0202270.
- [30] A.H. Mueller, Lectures given at the International Summer School on Particle Production Spanning MeV and TeV Energies (Nijmegen 99), Nijmegen, Netherlands, 8-20, Aug 1999, hep-ph/9911289.
- [31] A. Kovner, L.D. McLerran, H. Weigert, Phys. Rev. **D 52**, 3809 (1995).
- [32] A. Kovner, L.D. McLerran, H. Weigert, Phys. Rev. **D 52**, 6231 (1995).
- [33] Yu.V. Kovchegov, D.H. Rischke, Phys. Rev. **C 56**, 1084 (1997).
- [34] M. Gyulassy, L.D. McLerran, Phys. Rev. **C 56**, 2219 (1997).
- [35] Yu.V. Kovchegov, A.H. Mueller, Nucl. Phys. **B 529**, 451 (1998).
- [36] A. Krasnitz, R. Venugopalan, Phys. Rev. Lett. **84**, 4309 (2000).
- [37] A. Krasnitz, R. Venugopalan, Phys. Rev. Lett. **86**, 1717 (2001).
- [38] J.P. Blaizot, F. Gelis, R. Venugopalan, hep-ph/0402257.
- [39] E.A. Kuraev, L.N. Lipatov, V.S. Fadin, Sov. Phys. JETP **45**, 199 (1977).
- [40] I. Balitsky, L.N. Lipatov, Sov. J. Nucl. Phys. **28**, 822 (1978).
- [41] L.N. Lipatov, Sov. J. Nucl. Phys. **23**, 338 (1976).
- [42] V. Del Duca, hep-ph/9503226.
- [43] A. Dumitru, L.D. McLerran, Nucl. Phys. **A 700**, 492 (2002).
- [44] Yu.V. Kovchegov, K. Tuchin, Phys. Rev. **D 65**, 074026 (2002).
- [45] D. Kharzeev, Yu. Kovchegov, K. Tuchin, Phys. Rev. **D 68**, 094013 (2003).
- [46] M.A. Braun, Phys. Lett. **B 483**, 105 (2000).
- [47] A. Dumitru, J. Jalilian-Marian, Phys. Rev. Lett. **89**, 022301 (2002).

- [48] A. Dumitru, J. Jalilian-Marian, Phys. Lett. **B 547**, 15 (2002).
- [49] F. Gelis, A. Peshier, Nucl. Phys. **A 697**, 879 (2002).
- [50] F. Gelis, J. Jalilian-Marian, Phys. Rev. **D 67**, 074019 (2003).
- [51] B.Z. Kopeliovich, Phys. Rev. **C 68**, 044906 (2003).
- [52] D. Kharzeev, E. Levin, L.D. McLerran, Phys. Lett. **B 561**, 93 (2003).
- [53] R. Baier, A. Kovner, U.A. Wiedemann, Phys. Rev. **D 68**, 054009 (2003).
- [54] J. Jalilian-Marian, Y. Nara, R. Venugopalan, Phys. Lett. **B 577**, 54 (2003).
- [55] J.L. Albacete, N. Armesto, A. Kovner, C.A. Salgado, U.A. Wiedemann, hep-ph/0307179.
- [56] L.D. McLerran, R. Venugopalan, Phys. Lett. **B 424**, 15 (1998).
- [57] I.P. Ivanov, N.N. Nikolaev, W. Schafer, B.G. Zakharov, V.R. Zoller, hep-ph/0212176.
- [58] A. Accardi, M. Gyulassy, Contribution to the 19th Winter Workshop on Nuclear Dynamics, Breckenridge, USA, February 2003, nucl-th/0304083.
- [59] A. Krasnitz, Y. Nara, R. Venugopalan, Nucl. Phys. **A 727**, 427 (2003).
- [60] A. Krasnitz, Y. Nara, R. Venugopalan, Phys. Rev. Lett. **87**, 192302 (2001).
- [61] T. Lappi, Phys. Rev. **C 67**, 054903 (2003).
- [62] D. Antreasyan, J.W. Cronin, H.J. Frisch, M.J. Shochet, L. Kluberg, P.A. Piroue, R.L. Sumner, Phys. Rev. Lett. **38**, 112 (1977).
- [63] L. Kluberg, P.A. Piroue, R.L. Sumner, D. Antreasyan, J.W. Cronin, H.J. Frisch, M.J. Shochet, Phys. Rev. Lett. **38**, 670 (1977).
- [64] J.W. Cronin, H.J. Frisch, M.J. Shochet, J.P. Boymond, R. Mermoud, P.A. Piroue, R.L. Sumner, Phys. Rev. **D 11**, 3105 (1975).
- [65] A. Krzywicki, J. Engels, B. Petersson, U. Sukhatme, Phys. Lett. **B 85**, 407 (1979).
- [66] J.W. Qiu, G. Sterman, Nucl. Phys. **B 353**, 105 (1991).
- [67] J.W. Qiu, G. Sterman, Nucl. Phys. **B 353**, 137 (1991).
- [68] A. Ayala, J. Jalilian-Marian, L.D. McLerran, R. Venugopalan, Phys. Rev. **D 52**, 2935 (1995).
- [69] A. Ayala, J. Jalilian-Marian, L.D. McLerran, R. Venugopalan, Phys. Rev. **D 53**, 458 (1996).

- [70] E.M. Levin, K. Tuchin, Nucl. Phys. **B 573**, 833 (2000).
- [71] M.A. Braun, hep-ph/0101070.
- [72] N. Armesto, M.A. Braun, Eur. Phys. J. **C 20**, 517 (2001).
- [73] E. Iancu, K. Itakura, L.D. McLerran, Nucl. Phys. **A 724**, 181 (2003).
- [74] K. Rummukainen, H. Weigert, hep-ph/0309306.
- [75] K. Golec-Biernat, M. Wüsthoff, Phys. Rev. **D 59**, 014017 (1999).
- [76] K. Golec-Biernat, M. Wüsthoff, Phys. Rev. **D 60**, 114023 (1999).
- [77] F. Gelis, A. Peshier, Nucl. Phys. **A 707**, 175 (2002).
- [78] R. Venugopalan, Acta Phys. Polon. **B 30**, 3731 (1999).
- [79] E. Iancu, K. Itakura, S. Munier, hep-ph/0310338.
- [80] C.S. Lam, G. Mahlon, Phys. Rev. **D 62**, 114023 (2000).
- [81] E. Iancu, K. Itakura, D. Triantafyllopoulos, private communication.